6-25-2009

Synergy and Resistance Mechanisms in R115777 and PS-341 Models of Myeloma and Leukemia

Robert William Buzzeo
University of South Florida

Synergy and Resistance Mechanisms in R115777 and PS-341 Models of Myeloma and Leukemia

by

Robert William Buzzeo

A thesis submitted in partial fulfillment
of the requirements for the degree of
Masters of Science
Department of Biology
College of Arts and Sciences
University of South Florida

Major Professor: Patrick Bradshaw, Ph.D.
Richard Pollenz, Ph.D.
Kristina Schmidt, Ph.D.

Date of Approval:
June 25, 2009

Keywords: Tipifarnib, 8226/R5, Velcade, Farnesyl Transferase, Proteasome

Dedication

Dedicated to my family for their support and R.C. & Seamore for teaching me the true meaning of patience

Acknowledgments

I wish to thank Patrick Bradshaw, Richard Pollenz, Darren Beaupre, Melissa Alsina, Lori Hazlehurst, Nirangan Yanamandra, Javier Cuevas and William S. Dalton for their intellectual support.

I thank Paul Mackley and Yelenis Herrera for their technical support.

I thank Patrick Bradshaw, Richard Pollenz, Brian Livingston, Phil Wong, Nancy Wong and Lia Perez for their kind support

This research was supported in part by the following grants:

American Heart Association Greater Southeastern Affiliate Grant-In-Aid (0655291B, JC)

MMRF senior research grant and a Myeloma Research Foundation Grant

NIH grant: Clinical Scholars in Oncology 5K12 CA 87989-02
(D.M. Beaupre).

NIHClinical Scholars in Oncology grant 5K12 CA 87989-02 (D.M.
Beaupre and L.E. Perez)

Moffitt Aging and Cancer Pilot Research grant program
P20 CA103676 (D.M. Beaupre)

Leukemia Research Foundation New Investigator Award (D.M. Beaupre)

Table of Contents

List of Tables

List of Figures

Synergy and Resistance Mechanisms in R115777 and PS-341 Models of Myeloma and Leukemia

Robert W. Buzzeo

ABSTRACT

The farnesyl transferase inhibitor R115777 (Zarnestra, Tipifarnib) has been found to have clinical activity in diverse hematopoietic tumors. Clinical efficacy, however, does not correlate with Ras mutation status or inhibition of farnesyl transferase. To further elucidate the mechanisms by which R115777 induces apoptosis and to investigate drug resistance, we have identified and characterized a R115777-resistant human myeloma cell line. 8226/R5 cells were found to be at least 50 times more resistant to R115777 compared with the parent cell line 8226/S. 8226/R5 cells were insensitive to a diverse group of antitumor agents including PS-341 (Bortezomib, Velcade). Comparison of gene expression profiles between resistant and sensitive cells revealed expression changes in several genes involved in myeloma survival and drug resistance.

Identification and characterization of the 8226/R5 cell line helped us evaluate and confirm that the Akt tumor survival pathway plays an important role in Tipifarnib induced apoptosis and resistance in myeloma cells. Additionally, 8226/R5 cells helped to evaluate other molecules exhibiting synergistic cell death. In this study, we investigated the activity of R115777 combined with Bortezomib in microenvironment models of multiple myeloma and AML. The combination proved to be synergistic in multiple

myeloma and AML cell lines treated in suspension culture. Even in tumor cells relatively resistant to Tipifarnib, combined activity was maintained. Of importance, activation of the endoplasmic reticulum stress response was enhanced and correlated with apoptosis and reversal of CAM-DR. Our study provides the preclinical rationale for trials testing the Tipifarnib and Bortezomib combination in patients with multiple myeloma and AML.

Chapter 1

Introduction and Background

1.1 Multiple myeloma

Multiple myeloma (MM) also called Kahler's disease is a B cell malignancy in which no curative therapy exists. The disease was first characterized by Otto Kahler in the 19th century. Only 32% of individuals diagnosed with MM survive for more than 5-years (Dominik et al. 2007). The high mortality rate coupled with a painful disease state makes this cancer one of the more aggressive and harmful hematologic malignancies (Kyle et al. 2004).

The pathogenesis of this disease is not well understood however genes involved in cell cycle control (cyclin D) and apoptosis (Akt) have been implicated. DNA translocations involving chromosomes 13 and 14 have also been noted (Badros et al. 2007). Malignant B-cells will over-secrete the cytokine Interleukin-6 making the bone marrow microenvironment more suitable for tumorgenesis. Additionally the marrow becomes more vascular due to the tumor cells producing a protein known as VEGF (Badros et al. 2007).

Diagnosis of MM is made through the use of an ELISA evaluating the levels of M-Protein which is a specific protein secreted by a rapidly proliferating B cell (Dominik

et al. 2004). Monoclonal Gammopathies of Undetermined Significance (MGUS) is the hypothesized precursor to multiple myeloma. In this pre-disease state patients display a very low level of M-protein in the serum, however this level spikes during active disease (Kyle et al. 2004). Patients with multiple myeloma typically present with bone weakness, hypercalcemia and renal damage all related to the destruction of the skeleton. Additionally, individuals may exhibit immunocompromised characteristics and anemia because of damage or eventual ablation of the bone marrow (Kyle et al 2004).

Multiple myeloma is a relatively uncommon disease and thus epidemiological studies have shown to be difficult. About 15,000 new cases of MM have been diagnosed each year since 2002 (Dominik et al. 2004). The disease is most common in men and the elderly (> 40 yrs). It accounts for 15% of all hematopoietic malignancies or 2% of all the cancers in the United States. Importantly, the disease is almost 2 times more common in African Americans and 2 times less prevalent in those of Asian descent (Dominik et al. 2004). Cohort studies have identified a notable link between obesity and multiple myeloma, however the pathophysiology of this connection remains elusive. Other linkage factors including tobacco and aclochol abuse are beginning to be evaluated (Dominik et al. 2004).

Current therapy for MM includes stem cell transplants and chemotherapy. Autologous stem cell transplants have been proven to increase survival time following chemotherapy. Many chemotherapeutic compounds induce a state of aplastic anemia in which the bone barrow has been ablated. To compensate for this, autologous stem cells have shown to decrease the morbidity rates of anemia (Kyle et al. 2004).

Interestingly and probably as a result of the high mortality rate of MM, chemotherapeutic treatments now include drugs which target-specific proteins involved in the pathogenesis of MM. Clincial trials for MM are relatively quickly approved because of the poor prognosis of those with active disease (Kyle et al. 2004). Before 2005, the drugs which were used for treatment included the DNA damaging drugs Melphalin and Doxorubicin (Badros et al. 2007). In 2005 the FDA approved the use of Bortezomib; a proteosome inhibitor for the treatment of MM (Badros et al. 2007). The proteosome is a large protein complex responsible for degrading proteins in the cell. Hence, the proteosome is an essential part of protein regulation. Many of these proteins that are degraded are used by the cell to decrease proliferation and increase apoptosis – two opposite hallmarks of cancer. Laboratory studies have shown that the proteosome becomes hyperactive in cancer cells most especially (Palumbo et al. 2008). Thus as predicted proteosome inhibitors have exhibited fewer side effects in patients. This form of target specific therapy is a relatively new and exciting area of research and treatment. Regardless, tumor cells eventually succumb to resistance to many of these drugs, and patients relapse (Kyle et al 2004). As such the characterization and identification of compounds that can prevent the disease altogether remains crucial. Many drugs that inhibit oxidative cellular damage and help control oncogenic proteins or prevent DNA damage have been investigated (Badros et al 2007)

1.2 Drug resistance in Multiple Myeloma

Myeloma patients exhibit an initial response to chemotherapy but ultimately succumb to drug resistance. Unresponsiveness to a wide spectrum of anti-cancer agents is known as multidrug resistance (MDR) (Damiano et al. 1999). Two subsets of drug resistance have been characterized. *De novo* drug resistance includes the mechanisms that increase survival and contribute to the intital resistance of the drug-naïve tumor. Aquired resistance occurs over a period of time while the tumor is exposed to the chemotherapeutic agent. Aquired resistance is frequently correlated to gene mutation(s). Many types of *de novo* resistance have been well characterized including cell adhesion mediated drug resistance (CAM-DR) and environmental mediated drug resistance (EM-DR) (Li et al. 2005). The phenomenom of CAM-DR involves the interaction between the tumor cells and other cells in the bone marrow microenvironment, more specifically by contact of integrens to the substrate fibronectin (FN). EM-DR has been identified as a resistance type caused by soluble factors including those produced by autocrine and paracrine loops of the tumor cells. Additionally, resistance caused by factors released by bone marrow stromal cells is included in EM-DR type resistance (Li et al. 2005). As such, initial survival of the tumor cells via CAM-DR and/or EM-DR is more significant since it is the first step for tumor cells to escape drug death and eventually obtain acquired drug resistance (Li et al. 2005). The adhesion of cells to FN via integrins and subsequent cytotoxic protection has been well characterized as a substantial contributor to *de novo* drug resistance.

Fibronectin is an extra-cellular matrix (ECM) glycoprotein that binds to fibrin and collagen and is predominantly detected at contact sites between bone marrow stromal cells (BMSCs) (Van der Velde-Zimmermann et al. 1996**)**. Additionally fibronectin binds to class of adhesion molecules knows as integrins.

Integrins are a superfamily of adhesion molecules and are the best characterized for their role in regulating cell growth, differentiation and homing to the bone marrow (Hazlehurst et al. 2001). Integren receptors contain both α and β subunits and more than 25 of these subunits have been identified (Hazlehurst et al. 2001). β_1 integrins and fibronectin have been implicated in playing an important role in apoptotic suppression and cell survival (Damiano et el. 1999). FN adhesion through $\alpha_5\beta_1$ integrins induce increased expression of the antiapoptotic protein Bcl-2. This upregulation protected cells from serum starvation (Rozzo et al. 1997). Adhesion to fibronectin has been shown to protect myeloma RPMI 8226 cells from VP-16, radiation and front-line chemotheurpuetic drugs such as melphalan and doxorubicin (Hazlehurst et al. 2001). Importantly, β_1 integrins have been shown to activate multiple signal transduction pathways including FAK, MAPK, Src family kinases, PI3 kinase and AKT (Hanks et al. 1992, Lin et al. 1997, Meng et al. 1998, Lee et al. 2000, King et al. 1997). Many of the studies herein utilize FN adhesion so knowledge of their relevance to integrin signaling is of significant importance.

1.3 Farnysltransferase inhibitors and Ras proteins

Prenylation or isoprenylation is the addition of hydrophobic lipids to a protein. The three enzymes that prenylate proteins in the cell include farnesyltransferase (FTase), geranylgeranyltransferase (GGTase) and Rab geranylgeranyltransfeRase (Brunner et al. 2003). FTase adds a 15-Carbon isoprenoid lipid (farnesyl group) to the –SH of the cysteine of proteins which have a CAAX motif on their COOH termini. This type of post translational modification is termed farnesylation and is considered a type of prenylation event (Maurer-Stroh et al. 2003). Farnesylated proteins include the Ras superfamily of small GTP-binding proteins involved in the cell cycle regulation. Farnesylation causes the proteins to associate with the plasma membrane due to the hydrophobic nature of the farnesyl group. The Ras proteins are synthesized as cytosolic precursors that must associate with the cell membrane to transmit signals. Subsequently, membrane association can lead to heightened activation of these GTP-binding proteins. Farnesyl transfeRase inhibitors (FTIs) represent a novel class of cancer therapeutic drugs that are designed to inhibit the farnesylation of Ras protein.

The Ras superfamily of proteins is made up of 10 family proteins including Ras, Rho, Rab, Rap, Arf, Ran, Rheb, Rad, Rit and Miro (Munemitsu et al. 1990). They are implicated in cell proliferation, cytoskeletal dynamic, membrane trafficking, vasicular transport, nuclear transport, mitochondrial transport and the mTOR pathway. There are over 30 members of the Ras subfamily involved in cell proliferation. Three of these (H-Ras, K-Ras and N-Ras) are implicated in cancer when mutated and thus become

constitutively active. It has been well established that Ras mutations are not required for tumor cell succeptibility to FTIs (Brunner et al. 2003). However Ras mutations, most especially the N-Ras proto-oncogene, are detectable in ~15% of those diagnosied with myelodysplasia and 25% of those with acute myelogenous leukemia (Karp et al. 2001). As such targeting the activation of Ras for the treatment of hematopoetic malignancies presents as a sound approach to treatment.

Many FTIs have been synthesized. Some drugs are specific to FTase such as the drug primarily used in this study – R1125777 (Tipifarnib). However others have exhibited high efficacy in inhibiting GGTase as well. R115777 exhibited the highest level of specificity and lowest level of toxicity in pre-clinical models. Tipifarnib was submitted to the FDA by Johnson & Johnson for the treatment of AML in patients aged 65 and over however approval was rejected in June of 2005. However, Tipifarnib exhibited similar to lower toxicity ratings in a phase III clinical trial for the treatment of solid tumors (Cunningham et al. 2002, Van cutsem et al. 2002). Besides relatively low toxicity, FTIs have a distinct spectra of activity compared with classical chemotherapeutic agents. Additionally the growth inhibition by FTIs can supplement cytoxic effects of other drugs in an additive or synergistic way (Brunner et al. 2003). Because of these reasons, Tipifarnib should be considered a role in combination therapies for the treatment of certain tumors.

Chapter 2

Identification and Characterization of a R115777 Resistant Cell Line

Chapter 2 represents the following publication: Buzzeo et al. 2005

2.1 Introduction

Multiple myeloma is a plasma cell malignancy with no known curative therapy. RAS mutations occur frequently in myeloma (Bezieau et al. 2002, Hallek et al. 1998) and have been linked at least in some studies to a poor prognosis (Corradina et al. 1994, Bauduer et al. 1993, Liu et al 1996). Farnesyl transfeRase inhibitors (FTI) inhibit Ras function by preventing its posttranslational prenylation, a modification done by the enzyme farnesyl transfeRase (FTase). The FTI R115777 was designed as a highly selective inhibitor of FTase (End et al. 2001) and has been clinically tested in several hematopoietic tumors. This compound has shown activity in acute myelogenous leukemia, chronic myelogenous leukemia, and myelodysplastic syndrome (Karp et al. 2001, Cortes et al, 2003, Keating et al. 2002, Kurzrock et al. 2002)

Preclinical studies have reported that FTIs have antitumor activity in myeloma cell lines and primary isolates (Beaupre et al. 2003, Le Gouill et al. 2002, Bolick et al.

2003). Based on these observations, a phase II clinical trial testing R115777 in patients with relapsed myeloma was conducted(Alsina et al. 2005). Forty-three patients with a median of four prior treatment regimens entered the study. R115777 was well tolerated and 64% of patients achieved disease stabilization. Of importance, RAS mutation and inhibition of farnesyl transfeRase did not correlate with clinical efficacy consistent with a prior observation that R115777 can induce apoptosis via a Ras-independent mechanism (Beaupre et al. 2004). In myeloma cells, R115777 activates multiple intrinsic proapoptotic cascades (Beaupre et al. 2004). However, the molecules and/or signaling pathways that trigger these events remain elusive. To further elucidate the mechanisms by which R115777 induces apoptosis and to investigate drug resistance, I have established and characterized a R115777-resistant human multiple myeloma cell line (8226/R5). This line is unlike a previously described R115777-resistant colon cancer line (Smith et al. 2002) for resistance is unrelated to the prenylation activity of the enzyme FTase. This finding correlates with our observation that 8226/R5 cells are insensitive to a diverse group of antitumor agents, including PS-341. In this study, I investigate and exclude several potential mechanisms of R115777 resistance. Using comparative gene expression profiling (between sensitive and resistant cells), I have identified expression changes in several genes implicated in myeloma survival and drug resistance. Further evaluation of these genes may lead to the identification of novel FTI targets or resistance mechanisms that are clinically relevant.

2.2 Materials and Methods

2.2.1 Cell lines and reagents

The RMPI 8226 human myeloma cell line was obtained from the American Type Culture Collection (Manassas, VA). 8226/LR5 and8226/Dox40 lines were developed in our laboratory and have been previously described (Hazlehurst et al. 2003, Dalton et al. 1986) Sensitive and resistant 8226 cells were grown in RPMI 1640 (Mediatech, Inc., Herndon, VA) supplemented with 10% fetal bovine serum (Omega Scientific, Inc., Tarzana, CA). The 8226/R5 cell line was established by continuous exposure of 8226 parental cells (8226/S) to increasing concentrations of R115777 for over 6 months. The established 8226/R5 line is maintained in 5 μmol/L R115777. 8226/R5 cells were grown in R115777-free supplemented medium for 2 weeks before experimentation. R115777 and [^{14}C]R115777 (specific activity 1.43 GBq/mMol, 3.68 MBq/mL) were kindly provided by David End (Johnson and Johnson Pharmaceutical Research and development, LLC, Titusville, NJ). PS-341 was provided by Millennium Pharmaceuticals, Inc. (Cambridge, MA) and FTI277 from Said M. Sebti (Moffitt Cancer Center and Research Institute, Tampa, FL). Additional drugs were purchased from the following vendors: doxorubicin hydrochloride, melphalan, and perillic acid (Sigma Chemical, St. Louis, MO); staurosporine and etoposide (A.G. Scientific, San Diego, CA); and tunicamycin (Calbiochem, San Diego, CA).Antibodies and Western blotting Antibodies were purchased from the following vendors: anti–K-Ras-2B (C-19; Santa

Cruz Biotechnology, Inc., Santa Cruz, CA); anti-HDJ-2 (NeoMarkers, Freemont, CA); anti-hsp90, anti-hsp70, anti-hsp27, and anti–glyceraldehyde-3-phosphate dehydrogenase (Stressgen Biotechnologies, San Diego, CA); and anti–a-tubulin (BD Biosciences, San Diego, CA). Western blotting was done as described (Beaupre et al. 2003). For the majority of experiments, lysates were harvested using radioimmunoprecipitation assay lysis buffer [150 µMol/L NaCl, 1% NP40, 0.5% deoxycholic acid, 0.1% SDS, and 50 µMol/L Tris (pH 8.0)]. For evaluation of hsp27, hsp70, hsp90, and glyceraldehyde-3-phosphate dehydrogenase, lysates were harvested using Baverian lysis buffer [150 µMol/L NaCl, 1% Triton X-100, 30 µMol/L Tris (pH 7.5), and 10% glycerin].

2.2.2 Analysis of cell growth, cell cycle arrest, and cell death

Degree of resistance was determined using the tetrazolium salt 3,4,5-dimethylazol-2-yl-2,5-diphenyl tetrazolium bromide (MTT; Sigma) reduction assay. 8226/S and 8226/R5 cells were plated into 96-well microtiter plates at a density of $5x10^4$ cells/mL in 200 µl of supplemented media. Cells were exposed to a broad range of drug concentrations (R115777 and PS-341) in replicates of four. After a 72-hour (R115777) or 48-hour (PS-341) incubation period at 37°C, 50 µl of 2 mg/ml MTT was added to each well and cells were incubated for an additional 4 hours. Plates were centrifuged for 5 minutes at 1,200 rpm in a Sorvall RT6000D table top centrifuge (Sorvall, Asheville, NC), supernatants were removed, and the water-insoluble product was dissolved in 100 µl of 100% DMSO (Sigma). Plates were shaken for 30 seconds and absorbance read at 540 nm

on a Wallac Victor-2 1420 Multilabel Counter (Perkin-Elmer, Torrance, CA). The number of surviving cells was expressed as a percentage: absorbance of the experimental sample/ absorbance of the control x 100. The IC_{50} of the drug was calculated by linear regression analysis using Excel software. Flow cytometric cell cycle analysis was done after propidium iodide staining as previously described (Beaupre et al. 2003). The presented histograms represent gating on live cells only. Apoptosis and cell death were evaluated by flow cytometry after Annexin V-FITC and propidium iodide staining as per the recommendations of the manufacturer (BioVision Research Products, Mountain View, CA). TO-PRO-3 (Molecular Probes, Eugene, OR) was substituted for propidium iodide in experiments where cells were treated with doxorubicin. Cell death was calculated as the sum of Annexin V-FITC and propidium iodide or TO-PRO-3–positive cells. Specific cell death was determined by subtracting background death in untreated samples. Determination of P-glycoprotein expression 8226/S, 8226/Dox40, and 8226/R5 cells were washed in PBS [0.8% NaCl, 0.02% KCl, 0.14% NA_2HPO_4, 0.02% KH_2PO_4 (pH 7.4)] and resuspended in 200 µl of ice-cold PBS containing 0.5 µg/ml anti–Pglycoprotein- FITC antibody (BD Biosciences) or 0.5 µg/mL isotype control antibody anti-dansyl IgG2b,n-FITC (BD Biosciences). Samples were incubated on ice for 1 hour in the dark, washed twice in PBS, and analyzed by flow cytometry.

2.2.3 R115777 accumulation and efflux

To quantitate cellular accumulation of [^{14}C]R115777, 8226/S and 8226/R5 cells were washed once in PBS and 1 x 10^6 cells were resuspended in 1 mL supplemented

media containing 5 µmol/L R115777 (1:2.5 dilution of [^{14}C]R115777 to cold R115777). Cells were incubated at 37°C for increasing time periods and were then washed three times in 10 mL ice-cold PBS. Cell pellets were resuspended in 1 mL PBS and transferred to scintillation vials containing 10 mL Scintisafe 30% scintillation fluid (Fisher Scientific, Pittsburgh, PA). Samples were analyzed on a L56500 multipurpose scintillation counter (Beckman Coulter, Fullerton, CA). Because drug accumulation occurred rapidly, cells were incubated in 5 µmol/L R115777 at decreasing dilutions (1:10, 1:2.5, 1:1) of [^{14}C]R115777 for 1 hour and samples were processed and analyzed as described above to confirm a dose-dependent accumulation of [^{14}C]R115777 in each cell line. For efflux experiments, 8226/S and 8226/R5 cells were washed once in PBS and 1 x 10^6 cells were resuspended in 1 mL supplemented media containing 5 µmol/L R115777 (1:2.5 dilution of [^{14}C]R115777 to cold R115777). Cells were incubated for 1 hour at 37°C and then washed three times in 10 mL PBS and placed in R115777-free supplemented media for increasing time periods. Samples were then processed and analyzed as described above. Because efflux of R115777 also occurred rapidly, cells were incubated with 5 µmol/L R115777 at increasing dilutions (1:1, 1:2.5, 1:10) of [^{14}C]R115777 for 1 hour and then washed and placed in R115777-free media for an additional hour. Samples were processed and analyzed as above to confirm a dose-dependent efflux of [^{14}C]R115777. Experiments with 8226/S and 8226/R5 lines were done in parallel.

2.2.4 Microarray analysis

2.2.4.1 Probe arrays.

The oligonucleotide probe arrays were the Affymetrix U133A human arrays. These arrays consist of 22,215 probe sets, which target known and suspected genes as well as a number of suspected splice variants. The U133A chips detect an estimated 15,000 well characterized human genes.

2.2.4.2 Sample processing for microarray analysis.

Five micrograms of total RNA derived from 8226/S, 8226/LR5, and 8226/R5 cells served as the mRNA source for microarray analysis. The polyadenylate RNA was specifically converted to cDNA and then amplified and labeled with biotin following the procedure initially described by Van Gelder et al. (Va Gelder et al. 2000). Hybridization with the biotin-labeled RNA, staining, and scanning of the chips followed the proscribed procedure outlined in the Affymetrix technical manual and has been previously described (Warrington et al. 2000).

Scanned output files were visually inspected for hybridization artifacts and then analyzed using Affymetrix Microarray Suite 5.1 software. Signal intensity was scaled to an average intensity of 500 before comparison analysis. The MAS 5.1 software uses a statistical algorithm to assess increases or decreases in mRNA abundance in a direct

comparison between two samples (Van Gelder et al. 2000, Warrington et al. 2000). This analysis is based on the behavior of 11 different oligonucleotide probes designed to detect the same gene. The software generates a P value for the likelihood that any perceived difference was due to chance. The P values for all probe sets were exported to a text file and all pairwise comparisons were then aligned in Excel. For the comprehensive analysis, $P < 0.05$ was identified as changed (increased or decreased) for each individual comparison. Two independent samples from 8226/S, 8226/LR5, and 8226/R5 cells were collected. The samples generated from the resistant cell line were compared with the sensitive lines in all possible combinations. Genes were ultimately selected if they were identified as increased in all eight comparisons or decreased in all eight comparisons.

2.3 Results

2.3.1 8226/R5 cells are resistant to R115777-induced growth arrest and cell death.

Continuous culture of 8226/S cells with increasing concentrations of R115777 established the 8226/R5 line. In cytotoxicity assays, 8226/R5 cells were at least 50 times more resistant to R115777 compared with parental 8226/S cells (Fig. 2.1A). The IC_{50} for the 8226/S line was 0.1 mol/L and that for the 8226/R5 line was 5.4 μmol/L. Cell cycle analysis revealed that R115777 induced G1 growth arrest in 8226/S cells and this effect was largely abolished in the 8226/ R5 line (Fig. 2.1B). 8226/R5 cells were also protected

from apoptosis at concentrations of R115777 as high as 20 μmol/L (Fig. 1C; data not shown). The observed resistance was stable because cells cultured in R11577-free conditioned media for several months continued to display the resistant phenotype. Relative to doxorubicin- (8226/Dox 40) and melphalan resistant (8226/LR5) isogenic lines, 8226/R5 cells were the most resistant to R115777 (Fig. 2.1C).

2.3.2 Resistance to R115777 does not correlate with K-Ras prenylation or farnesyl transfeRase activity.

To determine whether 8226/R5 cells were cross-resistant to other compounds that inhibit prenylation, cells were exposed to inhibitors of FTase and geranylgeranyl transfeRase I (GGTase I). Similar to our results with R115777, 8226/R5 cells were resistant to the specific FTase inhibitor FTI 277 (22) when compared with parental 8226/S cells (Fig. 2.1). In addition, resistance was maintained in the presence of perillic acid, a compound that inhibits both FTase and GGTase I (Fig. 2.1B; ref. 23). 8226 cells express K-Ras and harbor a codon 12 K-RAS mutation. Similar to our prior observation in U266 cells (Beaupre et al. 2004), K-Ras remained prenylated in both sensitive and resistant cells after R115777 treatment (Fig. 2.2C). Moreover, farnesylation of HDJ-2 (a protein that can be farnesylated but not geranylgeranylated) was inhibited in both lines (Fig. 2.2D). These results indicate that R115777 resistance does not correlate with the prenylation status of K-Ras or HDJ-2. Furthermore, the fact that HDJ-2 farnesylation can

be inhibited in 8226/R5 cells implies that mutation of FTase (the drug target) is not responsible for the development of resistance.

2.3.3 Resistance is not related to decreased accumulation of R115777.

Many 8226 lines that acquire drug resistance have elevated expression of P-glycoprotein. An example of this is the 8226/Dox 40 cell line that expresses high levels of membrane P-glycoprotein that participates in the doxorubicin-resistant phenotype (Dalton et al. 1986). As expected, 8226/Dox 40 cells were found to have a marked increase in surface P-glycoprotein expression when compared with parent 8226/S cells (Fig. 2.3A). 8226/R5 cells, however, had membrane levels that were similar to that noted for the 8226/S line (Fig. 2.3A). Because increased expression or activity of other membrane pumps may also produce a resistant phenotype, we investigated the influx and efflux of R115777 in both 8226/S and 8226/R5 cells. Influx of R115777 occurred rapidly in both lines and reached steady state within 15 minutes of incubation with radiolabeled R115777 (Fig. 2.3B). A dose-dependent increase in R115777 uptake was also observed (Fig. 2.3C) and both time- and concentration-dependent experiments revealed that R115777 uptake was increased in 8226/R5 cells compared with the parental line. With regard to R115777 efflux, intracellular R115777 decreased rapidly (within 15 minutes) in both sensitive and resistant cells in time-course experiments (Fig. 2.3D). Furthermore, a dose-dependent efflux of R115777 was noted with resistant cells retaining more R115777

compared with sensitive 8226/S cells (Fig. 2.3E). These results indicate that 8226/R5 resistance is not related to decreased influx or increased efflux of R115777.

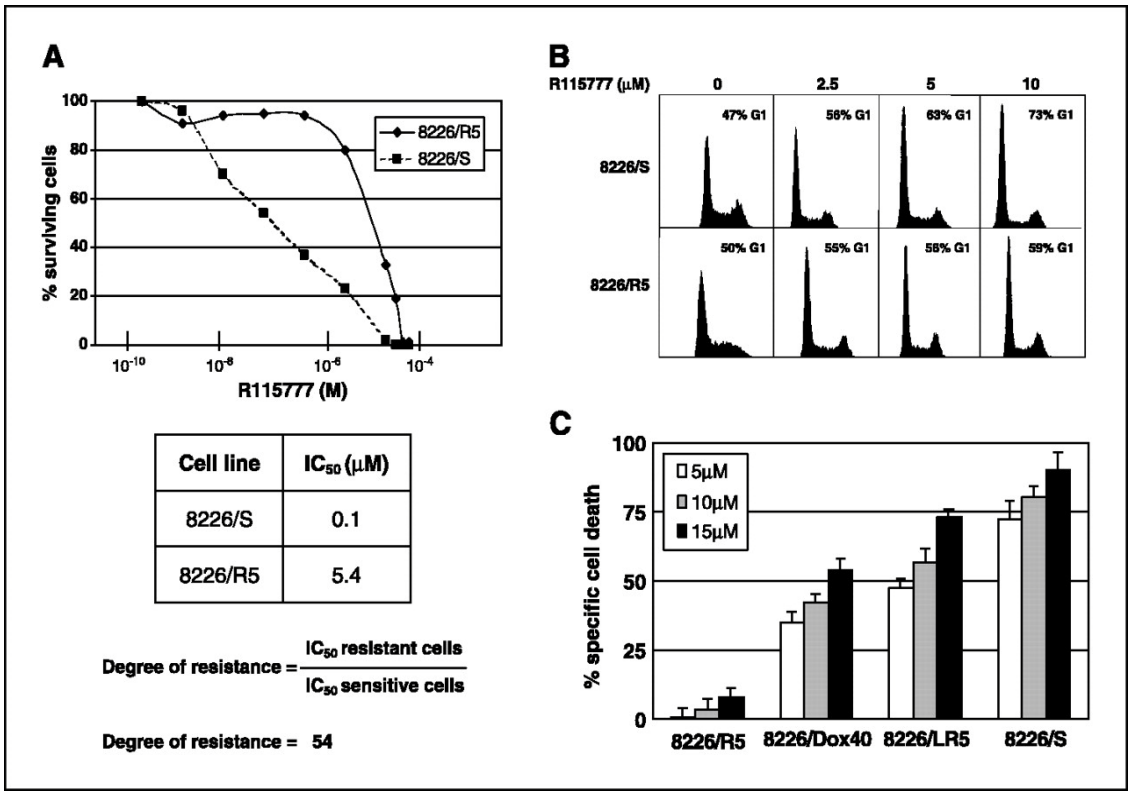

Cell line	IC_{50} (μM)
8226/S	0.1
8226/R5	5.4

$$\text{Degree of resistance} = \frac{IC_{50}\ \text{resistant cells}}{IC_{50}\ \text{sensitive cells}}$$

Degree of resistance = 54

Fig. 2.1. 8226/R5 cells are highly resistant to R115777. *A*, degree of resistance was determined using the MTT reduction assay. 8226/S and 8226/R5 cells were treated with increasing concentrations of R115777 for 72 hours. Percentage surviving cells was calculated relative to cells treated with control media only (see Materials and Methods). IC_{50} determinations were done by linear regression analysis. *B*, cell cycle analysis after R115777 treatment. Sensitive and resistant 8226 lines were treated with increasing concentrations of R115777 for 24 hours. Cell cycle arrest was determined by flow cytometry after propidium iodide staining. Gating was on live cells only. *C*, evaluation of cell death after R115777 treatment. 8226/S, 8226/Dox40, 8226/LR5, and 8226/R5 cells were treated with increasing concentrations of R115777 for 72 hours. Cell death was determined by flow cytometry after Annexin V-FITC and propidium iodide staining. Specific cell death was calculated by subtracting background death in untreated samples. The presented data is representative of three independent experiments.

2.3.4 8226/R5 cells display a multidrug-resistant phenotype and resistance is not associated with increased expression of heat shock proteins.

In an attempt to further categorize resistance, 8226/R5 cells were exposed to agents that induce apoptosis with diverse mechanisms of action. Compounds that have been reported to promote mitochondrial dysfunction, endoplasmic reticulum stress, and nuclear stress were tested (Fig 2.4 A-E) Surprisingly, 8226/R5 cells were resistant to all evaluated agents when compared with the parent 8226/S line. The proteosome inhibitor PS-341 has been shown to have cytotoxic activity in several chemoresistant myeloma lines (Ma et al. 2003). In cytotoxicity assays, 8226/R5 cells were three times more resistant to PS-341 when compared with 8226/S cells with an IC_{50} of 41.8 and 13.2 nmol/L, respectively (Fig. 2.5A). Unlike our findings with R115777, PS-341 induced G_2-M arrest in both sensitive and resistant cells with 8226/R5 cells being relatively protected (Fig. 2.5B). 8226/R5 cells were also protected from PS-341–induced apoptosis at concentrations as high as 20 nmol/L (Fig. 2.5C: data not shown). 8226/R5 cells maintained a PS-341–resistant phenotype when cultured in the absence of R11577 for several months, indicating stable resistance.

Heat shock proteins have antiapoptotic properties that can protect cells from stressful conditions. It has been previously reported that up-regulation of hsp70 can protect ovarian cancer cells from FTI-induced apoptosis (Hu et al. 2003). In addition, blockade of hsp27 expression has been shown to overcome PS-341 resistance in

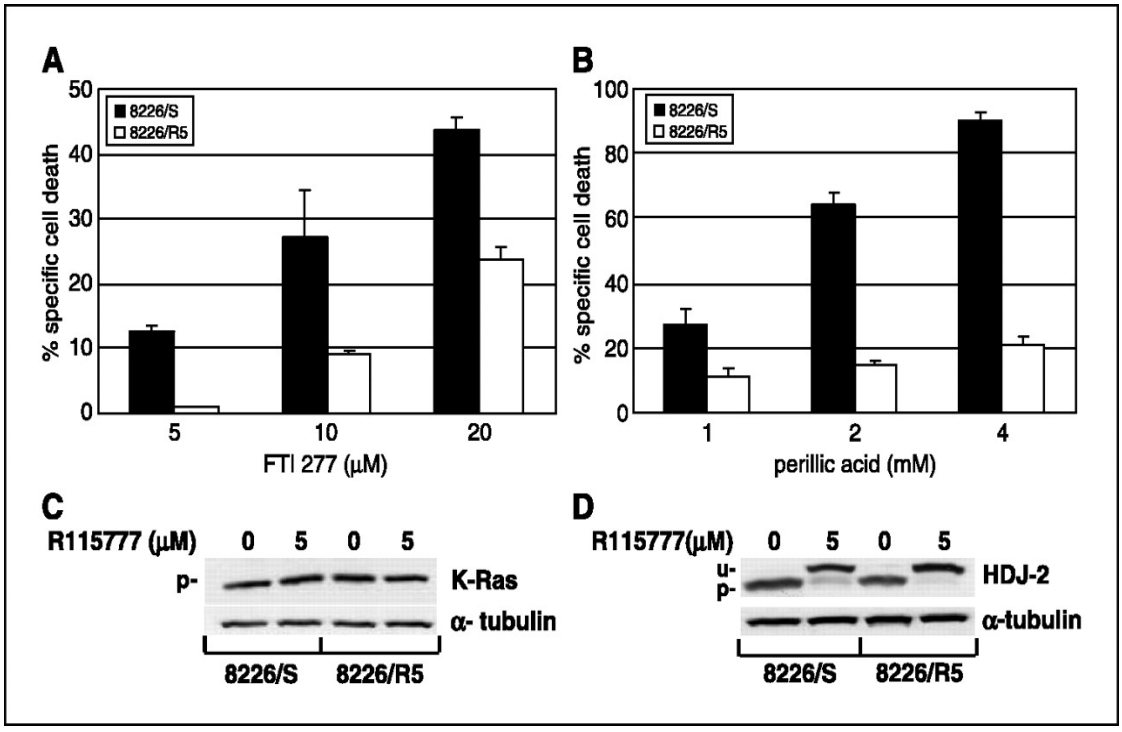

Fig. 2.2. Resistance in 8226/R5 cells is not linked to prenylation. A, 8226/R5 cells are resistant to the FTase-specific inhibitor FTI-277. 8226/S and8226 /R5 cellswere treated with increasing concentrations of FTI-277 for 72 hours. Cell death was determined by flow cytometry after AnnexinV-FITC and propidiumiodide staining. Specific cell death was calculated by subtracting background death in untreated samples. B, 8226/R5 cells are resistant to perillic acid, an inhibitor of both FTase and GGTase I. Sensitive and resistant cells were treated with increasing concentrations of perillic acid for 72 hours. Samples were analyzed as in (A). C, K-Ras remains prenylated in sensitive and resistant cells after R115777 treatment. 8226/S and8226 /R5 cells were treated with control media or 5 μmol/LR115777 for 72 hours. Cell lysates were harvested and evaluated by Western blotting using the indicated antibodies. D, HDJ-2 farnesylation is inhibited in both 8226/S and 8226/R5 cell lines. Sensitive and resistant cells were treated and analyzed as in (C) using the indicated antibodies. u, unprocessed form; p, processed form. (A) and (B) are representative of three independent experiments; (C) and (D) are representative of two independent experiments.

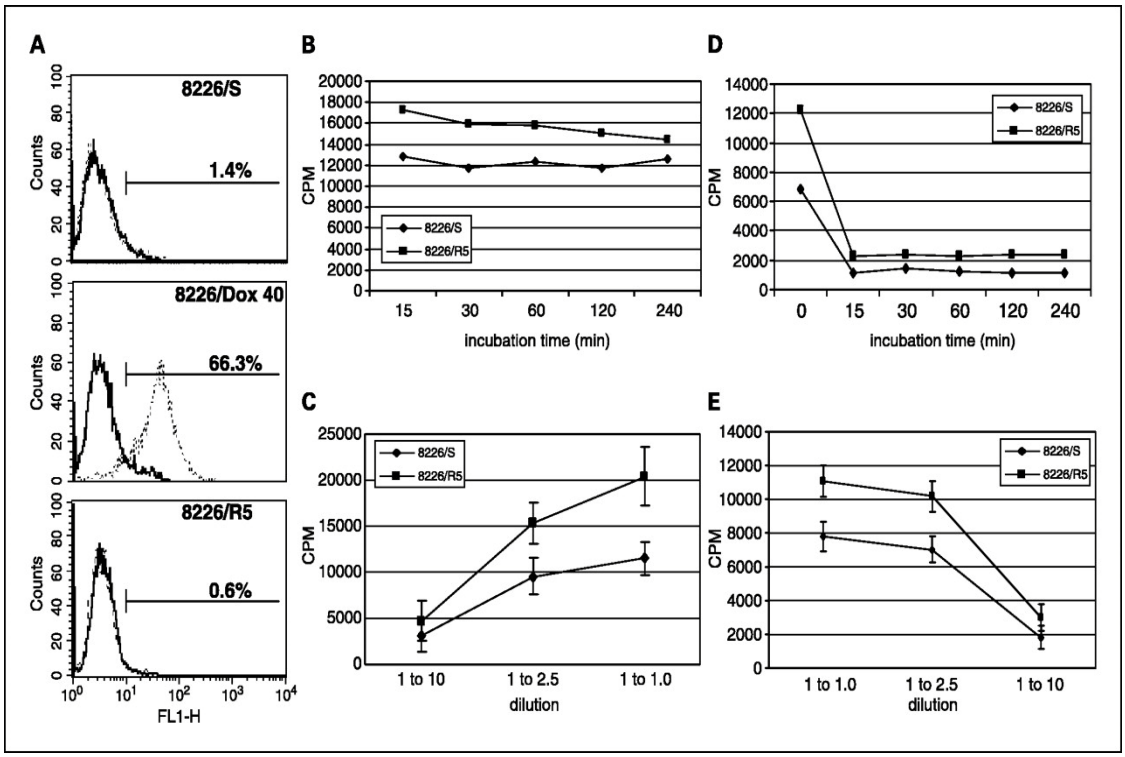

Fig. 2.3. Resistance is not related to decreased influx or increased efflux of R115777. A, P glycoprotein surface expression is not increased in 8226/R5 cells. 8226/S, 8226/Dox40, and 8226/R5 cells were stained with anti - P-glycoprotein (dashed line histograms) or isotype control antibody (solid line histograms) as described in Materials and Methods. Samples were analyzed by flow cytometry. Decreased accumulation and/or increased efflux of R115777 is not responsible for resistance in the 8226/R5 line (B-E). B, 8226/S and8226 /R5 cells were exposed to 5 µmol/LR115777 (1:2.5 dilution of [^{14}C]R115777 to coldR115777) in supplemented media for increasing time periods. Cells were washed and accumulation of [^{14}C]R115777 was quantitated by scintillation counting (see Materials and Methods). C, 8226/S and8226 /R5 cells were incubated in supplemented media containing 5 µmol/LR115777 at decreasing dilutions (1:10,1:2.5,1:1) of [^{14}C]R115777 for1hour. Samples were processed and analyzed as in (B) to confirm a dose-dependent accumulation of [^{14}C]R115777 in each line. D, sensitive and resistant lines were treated with 5 µmol/L R115777 (1:2.5 dilution of [^{14}C]R115777 to cold R115777) for 1 hour, then washed and placed in R115777-free supplemented media for increasing time periods. Samples were processed and analyzed as in (B). E, 8226/S and8226/R5 cells were treated with 5 µmol/LR115777 at increasing dilutions (1:1,1:2.5,1:10) of [^{14}C]R115777 for 1 hour and then washed and placed in R115777 free media for an additional hour. Samples were processed and analyzed as in (B) to confirm a dose-dependent efflux of [^{14}C]R115777. (A), (B), and(D) are representative of two independent experiments; (C) and (E) are representative of three independent experiments.

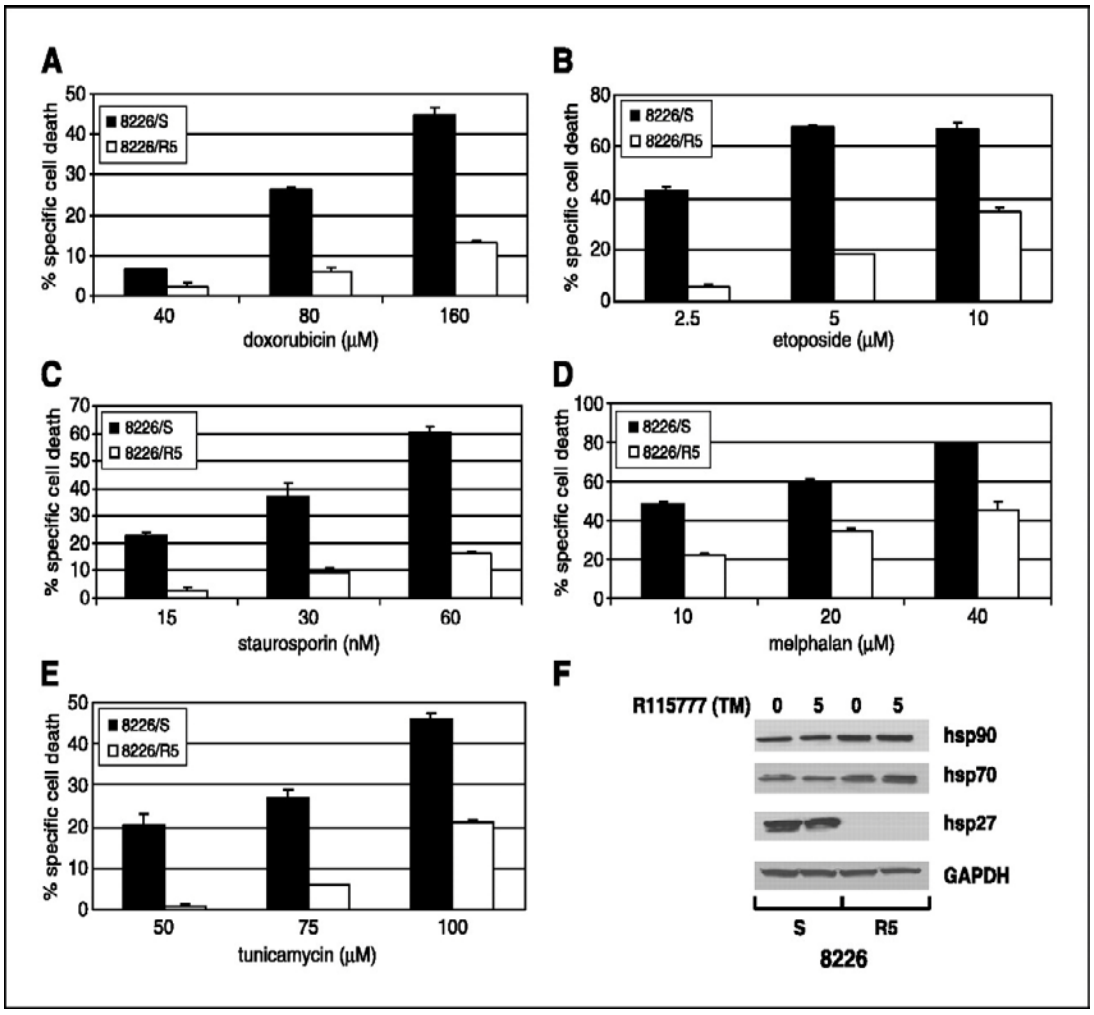

Fig. 2.4. 8226/R5 cells harbor a multidrug-resistant phenotype and resistance does not correlate with the expression of heat shock proteins. 8226/R5 cells display multidrug resistance (A-E). 8226/S and8226 /R5 lines were treated with the indicated compounds for 48 hours (A and B) or 24 hours (C-E). Cell death was determined by flow cytometry after Annexin V-FITC and propidiumiodide staining. Specific cell death was calculated by subtracting background death in untreated samples. The presented data is representative of three independent experiments. F, resistance in 8226/R5 cells is not associated with increased expression of heat shock proteins. 8226/S and8226 /R5 cells were treated with control media or 5 μmol/L R115777 for 72 hours. Cell lysates were harvested and analyzed by Western blotting using the indicated antibodies (see Materials and Methods). The presented data is representative of two independent experiments.

lymphoma cell lines (Chauhan et al. 2003, Chauhan et al. 2004). To determine whether multidrug resistance was related to overexpression of heat shock proteins, sensitive and resistant 8226 lines were evaluated for heat shock protein expression (Fig. 2.4F).

Expression levels of hsp70 and hsp90 were similar in sensitive and resistant lines and treatment with R115777 (drug-induced stress) had no appreciable effect. Hsp27 expression was also not effected in 8226/S cells after R115777 treatment but was undetectable in the 8226/R5 line. These results indicate that resistance does not correlate with the expression of heat shock proteins hsp27, hsp70, and hsp90.

2.3.5 Transcriptional profile of 8226/R5 cells.

To identify potential targets of R115777 and/or molecules associated with R115777 resistance, we compared gene expression profiles between sensitive and resistant variants of 8226 cells. Direct comparisons were made between the 8226/S and 8226/R5 cell lines. In an attempt to reduce the number of nonspecific gene expression changes identified, comparisons were also made between 8226/LR5 (which possessed an intermediate degree of resistance to R115777) (Fig. 2.1C) and 8226/R5 cells. This approach produced 2,064 probe sets (representing 1,666 genes) with changes unique to the 8226/R5 line. A selected list of genes involved in cell survival and growth, maintenance of cell cytostructure, cell-microenvironment contact, cholesterol biosynthesis, and protein degradation are presented in (Table 2.1)

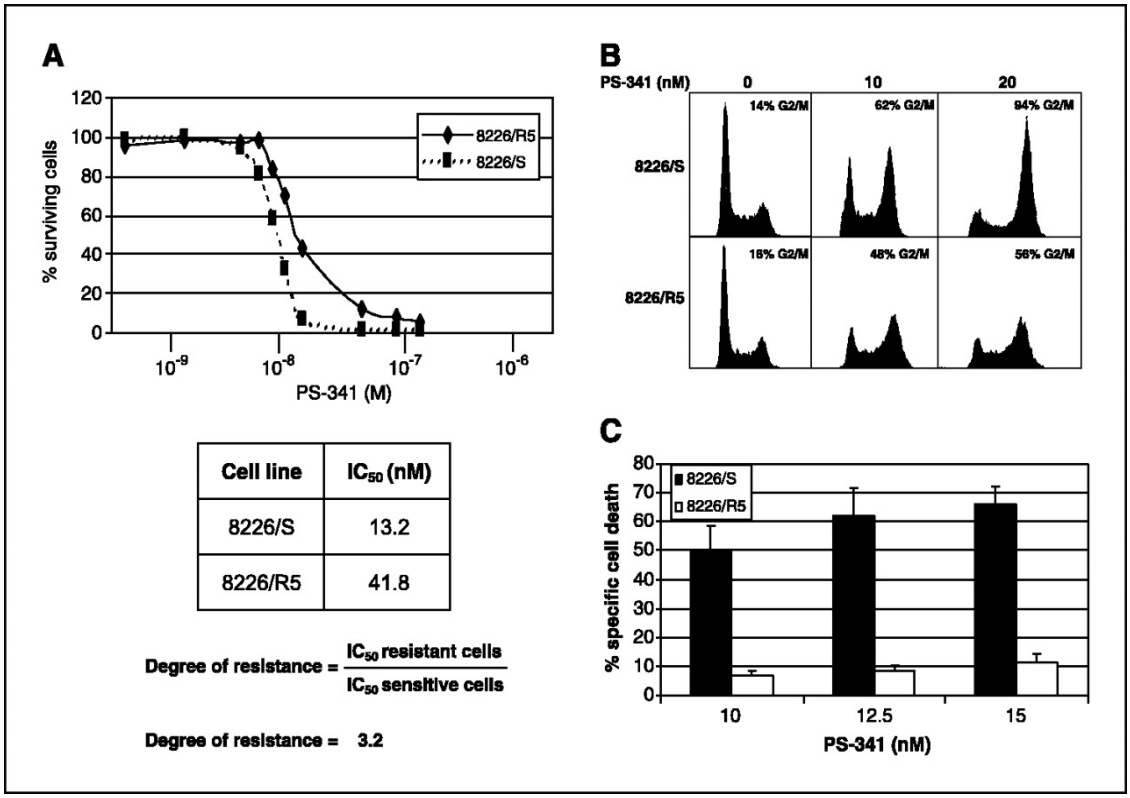

Cell line	IC_{50} (nM)
8226/S	13.2
8226/R5	41.8

$$\text{Degree of resistance} = \frac{IC_{50}\text{ resistant cells}}{IC_{50}\text{ sensitive cells}}$$

Degree of resistance = 3.2

Fig. 2.5 8226/R5 cells are resistant to PS-341. *A*, degree of resistance was determined by the MTT reduction assay. 8226/S and 8226/R5 cells were treated with increasing concentrations of PS-341 for 48 hours. Percentage surviving cells and IC_{50} determinations were done as in Fig 2.1. *B*, analysis of cell cycle after PS-341 treatment. Sensitive and resistant 8226 lines were treated with increasing concentrations of PS-341 for 24 hours. Cell cycle arrest was determined by flow cytometry after propidium iodide staining. Gating was on live cells only. *C*, evaluation of cell death after PS-341 treatment. 8226/S and 8226/R5 cells were treated with increasing concentrations of PS-341 for 48 hours. Cell death was determined by flow cytometry after Annexin V-FITC and propidium iodide staining. Specific cell death was calculated by subtracting background death in untreated samples. The presented data is representative of three independent experiments.

Expression Increased	Expression Decreased
Janus Kinase 2	Interleukin-6 receptor
Signal transducer and activator of transcription 1	Insulin-like growth factor 2 receptor
Bcl-XL	Mcl-1
Phosphoinositide-3-kinase	HSP27
FGFR activating protein 1	Retinoblastoma 1
Fibroblast growth factor 20	Transforming growth factor
Mavalonate kinase	Tumor protein p53
Rap 2A	Farnesyl diphosphate synthetase
Rab GGase, B-subunit	Lamin A/C
Rab 4A	Ras protein activator like-1
Ras and Rab interactor 3	Ras and Rab interactor 2
Mitogen-activated protein Kinase 1	Rab 36
Mitogen-activated protein kinase 9	Rho GTPase-activating protein 6
Mitogen-activated protein kinase 14	Mitogen-activated protein kinase phosphatase
Cyclin D3	Cyclin D1
Fas apoptotic inhibitory molecule	Syndecan 1
Calmodulin 3	X-box-binding protein 1
Calpain 2	Beta-Actin
S100 calcium binding protein A13 and A14	Fibronectin-1
Collagan type XXI	Integrin B5
Paxillin	Integrin B7
Integrin-4	Ubiquitin-conjugating enzymes
Proteosome inhibitor subunit 1	A100 calcium binding protein (A11 calgizzarin)

Table 2.1 Gene expression changes in 8226/R5 cells

2.4 Discussion

FTIs were designed as specific inhibitors of Ras intended to interfere with a crucial posttranslational processing step. Ras requires the addition of a 15-carbon farnesyl group to its carboxyl-terminal cysteine, which permits its localization to the plasma membrane (a requirement for function). This modification is done by the enzyme FTase, the purported target of R115777. It has been well established that alternate prenylation of Ras may occur in the presence of FTIs (Sebti et al. 2000). This has been most notably described for K-Ras but also applies to the N-Ras protein. These reports are consistent with our prior observation in U266 cells (N-Ras–expressing line; ref. Beaupre et al. 2004) and our present finding that K-Ras remains prenylated in 8226/S cells after R115777 treatment. These results suggest a Ras-independent mechanism of cell death. This is further supported by the clinical observation that responses to R115777 do not correlate with Ras mutation status or inhibition of farnesyl transfeRase measured *ex* vivo (Karp et al. 2001)Karp et al. 2001, Kurzrock et al. 2003, Alsina et al. 2004).

We hypothesized that the isolation of a R115777-resistant human myeloma cell line (8226/R5) might provide insight concerning the potential targets of R115777 or identify novel mechanisms of FTI resistance. R115777 resistance was not associated with an increase in the surface expression of P-glycoprotein nor was it associated with decreased influx or increased efflux of R115777. In addition, the expression of heat shock proteins (hsp27, hsp70, hsp90) did not correlate with the drug-resistant phenotype. We therefore undertook molecular profiling of sensitive and resistant 8226 lines and

identified expression changes in several genes implicated in cell survival and drug resistance. They included genes involved in cell signaling, cholesterol biosynthesis, and protein degradation. It remains possible that molecules associated with one of these genes is a major target of R115777 and/or directly participates in FTI resistance.

Our microarray data identified increased expression of several proteins associated with Jak-Stat signaling, including Jak2. In primary isolates, constitutive Stat3 activation has been observed in the majority of patients with multiple myeloma (Catlette-Falcone et al. 1999, Bharti et al. 2004. Stat3 homodimers and Stat1:Stat3 heterodimers seem to be the predominant DNA-binding forms (Catlette-Falcone et al. 1999). It has been reported that inhibition of Stat3 can sensitize resistant myeloma cells to chemotherapy mediated apoptosis (Alas et al. 2003). These results imply that Jak-Stat signaling may contribute to the drug-resistant phenotype. Stat3 activity has been linked to up-regulation of Bcl-X_L (Catlette-Falcone et al. 1999) and consistent with this, Bcl-X_L expression was increased in 8226/R5 cells. Elevated expression of Bcl-X_L has been observed in several hematopoietic tumors, including blast crisis chronic myelogenous leukemia and non-Hodgkin's lymphoma (Grad et al. 2000), and one study suggested that it was an indicator of chemoresistance in multiple myeloma (Tu et al. 1998). We have previously reported that R115777 can partially overcome drug resistance in U266 cells that maintain high levels of stable Bcl-X_L expression (Beaupre et al. 2004). These findings imply that R115777 resistance may only in part be regulated by increased Jak-Stat signaling or Bcl-X_L expression in 8226/R5 cells.

Our comparative gene expression profiling also identified other genes potentially involved in R115777 resistance. Phosphatidylinositol 3-kinase is a heterodimer consisting of p85 and p110 subunits (Otsu et al. 1991, Hiles et al. 1992). The p110 δisoform is preferentially expressed in cells of hematopoietic origin (Chantry et al. 1997, Vanhaesebroeck et al. 1997) and elevated expression of the catalytic δpolypeptide was observed in the 8226/R5 line. An important downstream target of phosphatidylinositol 3-kinase is Akt/protein kinase B, a protein that is known to play a role in myeloma survival and drug resistance (Hideshima et al. 2001, Tu et al. 2000, Hsu et al. 2002). Interestingly, it has been reported that FTI-induced apoptosis can be prevented by a constitutively activated form of Akt-2 (Jiang et al. 2000). Therefore, it remains possible that phosphatidylinositol 3-kinase/Akt signaling also contributes to R115777 resistance and the multidrug-resistant phenotype. Because the p110 δsubunit is mainly expressed in hematopoietic cells, it potentially represents a novel therapeutic target particularly for resistant tumors of hematopoietic origin.

Our analysis also identified increased expression of mevalonate kinase, an enzyme associated with cholesterol biosynthesis. Influx and efflux experiments suggest that R115777 is retained in 8226/R5 cells compared with the parent 8266/S line. This is relevant because an increase in cholesterol-rich microdomains, such as lipid rafts, have been associated with the development of multidrug resistance (Lavie et al. 2000). R115777 is a lipophilic molecule that could potentially be sequestered and compartmentalized in such microdomains; however, in 8226/R5 cells, R115777 efficiently inhibits FTase. Nevertheless, it remains possible that subcompartmentalization

of R115777 influences its interaction with unforeseen targets. Also of importance was the observation that 8226/R5 cells were resistant to the proteosome inhibitor PS-341. It has been previously reported that increased expression of hsp27 produces a PS-341–resistant phenotype in multiple myeloma cells (Chauhan et al. 2003). In 8226/R5 cells, however, hsp27 protein expression was undetectable. Our microarray analysis revealed decreased expression of the 26S proteosome subunit (the target of PS-341) in 8226/R5 cells when compared with the parental 8226/S line. This perhaps represents a novel mechanism of proteosome inhibitor resistance.

In conclusion, I have identified a myeloma cell line with resistance to both R115777 and PS-341. Further characterization of this line may lead to identification of novel drug targets or resistance mechanisms that are clinically relevant.

Chapter 3

The Akt Pathway plays an Important Role in R115777 Induced Apoptosis and Resistance in Multiple Myeloma

3.1 Introduction

Multiple myeloma (MM) is a malignant B-Cell neoplasm characterized by the proliferation of clonal plasma cells preferentially in the bone marrow (Hallek et al. 1998, Ghafoor et al 2002). While chemotherapy exhibits an initial response, patients eventually succumb to acquired drug resistance (Bergsagel et al. 1995, Dalton et al. 1997). Current research is focusing on identification of targets in the myeloma cell implicated in tumor cell growth, survival and drug resistance. This research has led to the development and study of innovative compounds such as thalidomide, immunomodulatory drugs (IMIDs) and proteasome inhibitors for the treatment of MM (Weber et al. 2003, Richardson et al. 2004, Pei et al 2004, Weber et al. 2002, Santucci et al 2003).

Ras mutations occur frequently in myeloma as then are found in 50% of patients with advanced disease (Neri et al. 1989). Furthermore, patients with mutated Ras are less likely to respond to chemotherapy and have a shorter median survival (Liu et al. 1996). Therefore, the development of compounds to inhibit Ras activity may exhibit antitumor activity in MM as well as other cancers. One such family of Ras-inhibiting agents is the

FarnesyltransfeRase inhibitors (FTIs) (Datlon et al. 1997). Ras prenylation is necessary for oncogenic activity. Prenylation is a post-translational addition of an isoprene lipid moiety at the cysteine residue in a consensus sequence (CAAX box) of the COOH terminus (Kato et al 1992, Willumsen et al. 1984, Hancock et al 1989, Sebti et al. 2000). Ras is preferentially prenylated by FarnesyltransfeRase (FTase), however GeranylgeranyltransfeRase (GGTase) will alternatively prenylate the k-Ras isoforms (Sebti et al. 1997, Sebti et al 2000, Sun et al. 1998). While early generation FTIs were designed as peptidomimetics of the CAAX box, current molecules are mostly non-peptide, non-thiol containing compounds with nanomolar potency including farnesyl pyrophosphate analogues and non-peptide compounds derived from high throughput screening (Cox et al, 2001). Tipifarnib, also known as FTI-R115777 or Zarnestra is a non-peptidomimmetic substituted quinoline inhibitor of the CAAX binding site of FTase (Hahn et al. 2001, Tamoni et al. 2001). *In vitro*, Tipifarnib has shown to inhibit the prenylation of lamin A in MCF-7 breast cancer cells (Kellard et al. 2001), and the prenylation of lamin B, H-Ras, and N-Ras in colon, pancreatic, and melanoma cell lines (End et al. 2001).

Tipifarnib treatment of patients with advanced myeloma in a phase II clinical trial exhibited disease stabilization in 64% of patients (Alsina et al. 2004). Of importance, RAS mutation status and inhibition of FTase did not correlate with clinical efficacy. This is consistent with prior observations that Tipifarnib can induce apoptosis via Ras-independent mechanisms (Beaupre et al. 2004). Interestingly, treatment with

Tipifarnib decreased levels of phosphorylated Akt (pAkt) and STAT3 in bone marrow from patients where these tumor survival pathways were constitutively active.

The serine/threonine kinase Akt is an important downstream target of phosphatidylinositol-3-kinase (PI3K) (Cantly et al. 2002). The PI3K/Akt signaling pathway is a key mediator of cell survival while interacting with pro-apoptotic proteins including Bad, and Caspase 9, as well as the anti-apoptotic protein IKK(Nrunet et al. 1999, Madrid et al. 2000)

The phase II clinical trial demonstrated disease stabilization in 2 out of 2 patients where Tipifarnib inhibited Akt phosphorylation. This suggests that either pAkt or an upstream kinase or modulator of pAkt may be targeted by Tipifarnib. These findings are consistent with those of other groups which indicate that the efficacy of FTIs anti-proliferative and apoptotic responses on tumor cells may be due to the drug affecting other proteins than Ras (Takada et al. 2004). It has been reported that the PI3-kinase/Akt pathway is a critical target for FTI-induced apoptosis in ovarian and pancreatic cancer cell lines and in Ras-transformed rodent fibroblasts, respectively (Du et al. 1999).

In MM primary isolates, Akt has been found to be predominately activated and localized to the nucleus (Alkan et al. 200). pAkt has show to be primarily localized to the nucleus following receptor activation in B lymphocytes (Tu et al. 2000). Additionally, activated Akt in the nucleus has been implicated in the modulation and activity of regulatory proteins including the Forkhead/FOXO family of transcription factors (Brunet et al. 1996). No direct correlation between Akt localization and drug resistance has yet been characterized. It has however been well established that Akt activation inhibits

transcription of RhoB (Jiang et al. 2000) and that RhoB controls Akt nuclear/cytoplasmic trafficking in retinal cells (Adini et al. 2003)

As such, we have examined the mechanisms of the cytotoxicity of Tipifarnib *in vitro* and *in vivo* and its correlation with the status of Akt activation. We have demonstrated that Tipifarnib induces apoptosis in a dose dependent manner in two out of three MM cell lines. Using a SCID-hu model of myeloma we show that Tipifarnib was cytotoxic to myeloma cells *in vivo*. Additionally, we have correlated levels of pAkt expression to Tipifarnib resistance with cell lines harboring higher levels of pAkt such as the Tipifarnib resistant RPMI-8226 cell line (8226/R5) (Buzzeo et al. 2005). Ectopic expression of constitutively active Akt in B-cells induces Tipifarnib resistance and we identify a correlation between nuclear localization of pAkt and drug resistance in MM cell lines. To this end, we can confirm that the Akt tumor survival pathway plays an important role in Tipifarnib induced apoptosis and resistance in myeloma cell lines.

3.2 Material and Methods

3.2.1 Cell culture

Myeloma cell lines RPMI-8226, and U266 were obtained from ATCC (Manassas, VA). The murine pro-B cell, Ba/F3 was obtained from DSMZ (Braunschweig, Germany). MM1.S cells were generously donated by Steven T. Rosen (Northwestern University, Chicago, Illinois). 8226/S and 8226/R5 cells have been previously characterized (Buzzeo

et al. 2005) and were developed in this lab. All cell lines were maintained in RPMI medium (CellGro, Mediatech, Herndon, VA) supplemented with 10% fetal bovine serum (FBS), 100 U/mL penicillin/streptomycin, and 100 μM L-glutamine (Gemini Bio-Products, Calabasas, CA). Medium for the IL-3 dependant Ba/F3 cells was supplemented with 10% WEHI conditioned medium. WEHI cells were obtained from ATCC and grown in RPMI supplemented with 10% FBS. Cells were grown to high confluency, and conditioned medium filtered through a 0.4μ filter. 8226/R5 cells were cultured in the presence of 5μM Tipifarnib however drug was removed two weeks prior to experimentation.

3.2.2 Drug preparation

Tipifarnib (FTI-R115777, Janssen Research Institute, Beerse, Belgium) was diluted in DMSO (Fisher Chemical, Pittsburg, PA) to a concentration of 5mM, sonicated 10 minutes in a water bath sonicator (Branson 3510) and stored at -20°C.

3.2.3 Proliferation assay

Half-log serial dilutions of Tipifarnib, from $5x10^{-10}$ to $5x10^{-6}$ M were plated in quadruplicate in 96 well plates. RPMI-8226, U266, and MM1.S cells in log phase growth were added at 10,000 cells per well (Ba/F3 cells at 5,000 cells/well) and incubated for 72 hours at 37^{o}C. 50μL of 2mg/ml 3-[4,5-Dimethyl-2-yl]-2,5 diphenyl-tetrazolium bromide

(MTT dye) (Sigma, St. Louis, MO) was added to each well. Plates were incubated an additional 4 hours and centrifuged at 1,200 rpm. The supernatant was aspirated, the precipitate solubilized in 100 μL DMSO and the plates were shaken for 30 seconds with sample absorbances read at 450nM. IC_{50} values were calculated by linear regression analysis of the dose response curve. Data shown represents an average of 3 independent experiments and includes standard error.

3.2.4 Apoptosis assay

Myeloma cells were grown 48 hours in the presence of vehicle control (DMSO), or varying concentrations of Tipifarnib. Cells were collected, washed in PBS, and stained with 5μl Annexin V-FITC (Clonetech, Palo Alto, CA) and 5μl Propidium Iodide (Clonetech, Palo Alto, CA) in 0.5 ml annexin binding buffer. Apoptosis was determined by Flow Cytometry and analyzed using CellQuest software (Becton Dickinson, Carpinteria, CA). Data shown represents an average of 3 independent experiments and includes standard error.

3.2.5 Immunostaining

For western blotting, cells were washed in PBS and lysed in Baverian lysis buffer (30 mM HEPES, pH 7.5, 10 mM NaCl, 1% Triton X-100, 10% glycerol, 5mM $MgCl_2$, 1 mM EGTA) with freshly added protease and phosphatase inhibitors (25 mM NaF, 25

μg/ml Leupeptin, 2mM phenylmethylsulfonylfluoride (PMSF), 2 mM sodium orthovanadate, 10 μg/ml soybean trypsin inhibitor, and 10 μg/ml aprotinin). Nuclear and cytoplasmic fractions were separated using NE-PER (Pierce, Rockford, IL.) per the manufacturer's instructions. 50 μg protein was run on 12.0% acrylamide gels and transferred to PVDF membranes (Millipore, Billerica, MA). Blots were blocked in 5% milk in 0.1% PBS-Tween for 2 hrs, incubated overnight in primary antibody in 5% BSA, washed for 45 min in 0.1% Tween and incubated for 1 hr in secondary antibody. The wash was repeated and bands were visualized using SuperSignal West Dura Extended Duration Substrate (Thermo Scientific). Antibodies were purchased from the following vendors: Caspase-3, Cleaved Caspase-3 (Asp175), Akt, pAkt(Ser473), pAkt(Ser473)–IHC Specific, HRP-anti-mouse and HRP-anti-rabbit (Cell Signaling Technologies, Danvers, MA); β-actin, ά-tubulin, GAPDH and anti-HA (Sigma Chemical, St. Louis, MO). Data shown is representative of three independent experiments.

For immunohistochemistry (IHC), 0.5 x 10^6 8226/S, 8226/R5 and MM1.S cells were cytospun and fixed in 4 % paraformaldehyde for 1 min, air dried and incubated in methanol for 5 min at -20°C. Slides were incubated in a 1:00 dilution in Tris Bufferred Saline (TBS) (3%BSA) with 1:100 diluted pAkt(Ser473)-IHC Specific antibody for 1 hr, and washed three times in TBS (10 min/wash). Slides were incubated with secondary at a dilution of 1:80 in TBS(1%BSA) for 1 hr, washed three times in TBS and incubated for 1 hr in avidin-biotin peroxidase complex (ABC reagent). Slides were then washed three times in TBS and incubated with DAB reagent (15 min) (Zymed Laboratories) then stained with or without Hematoxylin (2 min) (Zymed Laboratories). Cells were

visualized by light microscopy and captures are representative of three independent experiments.

3.2.6 Murine studies

To develop myeloma SCID-hu mice, C.B-17 mice homozygous for both the severe combined immunodeficiency (*scid*) and beige (*bg*) mutations (C.B-1 7/GbmsTac-*Prkdc*^{scid} *Lyst* ^{bg}, herein referred to as SCID; Taconic, Germantown, New York) were used. Human fetal bones of 18–23 weeks of gestation were obtained from Advance Bioscience Resource (Alameda, California) and from the General Hospital of Vienna (Vienna, Austria) in compliance with the regulations issued by the state and federal governments. SCID mice 6–8 weeks old were transplanted subcutaneously with fetal human bones (humerus, femur or tibia) and fetal thymus, as previously described(URashima et al. 1997). Six weeks post implant $5x10^4$ RPMI-8226 cells were injected directly into the implanted bones. Beginning at 10 weeks post-implant, and each week thereafter, urine was collected from 12 mice and tested for free λ-light chain immunoglobulin levels by Radial Immunodiffusion (BIND A RID-human kappa and lambda free, The Binding Site Limited, Birmingham, UK). At 12 weeks post-implant and after the presence of disease was established, Tipifarnib was administered by gastric lavage at a dose of 50 mg/kg/d, once per day for two weeks. At the conclusion of the drug course 10 mice were euthanized via decapitation and implanted bones were removed for

histology. Wright-Gimsa staining on all 10 bone sets were performed and evaluated by light microscopy.

3.2.7 Gene constructs, transfection and fluorescent microscopy

Constitutively active HA-Myr-Akt1 (Myr-Akt) was previously described (Frank et al. 1995), pDsRed2 (Clontech), pDsRed2-HA-Myr-Akt1 and pcDNA3 (Invitrogen) were generous gifts from Jin Cheng (University of South Florida, Tampa, Fl.). Ba/F3 cells were transfected using Nucleofection Solution-V (Amaxa Biosystems) according to the manufacturer's instructions. Cells were selected for 2 weeks in 300µg/ml G418 (Gibco Scientific). 5,000 cells were stained with DAPI + mounting medium (Vector Labs, Burlingame, CA) and viewed with a fully automated, upright Zeiss Axio-ImagerZ.1 microscope with a 63x /1.40NA oil immersion objective, and DAPI and Rhodamine filter cubes. Images were produced using the AxioCam MRm CCD camera and Axiovision (v.4.5).

3.3 Results

3.3.1 Tipifarnib induces apoptosis in RPMI-8226, and U266 myeloma cell lines, but not the MM1.S cell line.

MTT and Annexin-V binding assays were used to determine Tipifarnib sensitivity in three myeloma cell lines. MTT binds active mitochondrial reductase enzymes and its

resulting formazin product is associated with cellular proliferation and viability. Of the three cell lines examined RPMI-8226, and U266 cell lines had IC_{50}'s less than 5 μM, the manufacturer's recommended maximum dose for specific inhibition (Fig. 3.1A). RPMI-8226 cells were most sensitive (IC_{50}=64 nM) while U266 (IC_{50}=2.13 μM) and MM1.S (IC_{50}=12.2 μM) cells were increasingly more resistant. Notably, MM1.S cells exhibited an IC_{50} value 190 times greater than that of the RPMI-8226 cells.

Annexin-V binding indicated that the decrease in proliferation observed in MTT data was due to apoptosis, not growth arrest (Fig. 3.1B). Consistent with the MTT results the apoptosis assay showed the RPMI-8226 cells to be most sensitive, followed by U266 cells, with the MM1.S cells most resistant to Tipifarnib.

Expression of effector caspase (Caspase-3) cleavage was analyzed by western blotting (Fig 3.2A-B). A 48-hour time course with 1 μM Tipifarnib treating RPMI-8226 and MM1.S cells showed induction of caspase-3 activation in RPMI-8226 cells beginning at 24 and continuing through 48 hours. However, the same dose failed to do so in MM1.S cells (Fig 3.2A). After the appropriate time time of caspase cleavage was found, a dose dependent increase in Caspase-3 cleavage in RPMI-8226, and U266 cell lines following seventy-two hour treatment with 0.05, 0.5 or 5.0 μM Tipifarnib is observed(Fig 3.2A). A similar response was not observed in MM1.S cells. This data further substantiates the previous annexin data (Fig 3.1) that Tipifarnib is inducing apoptosis in cells sensitive to it, while MM1.S cells remain resistant.

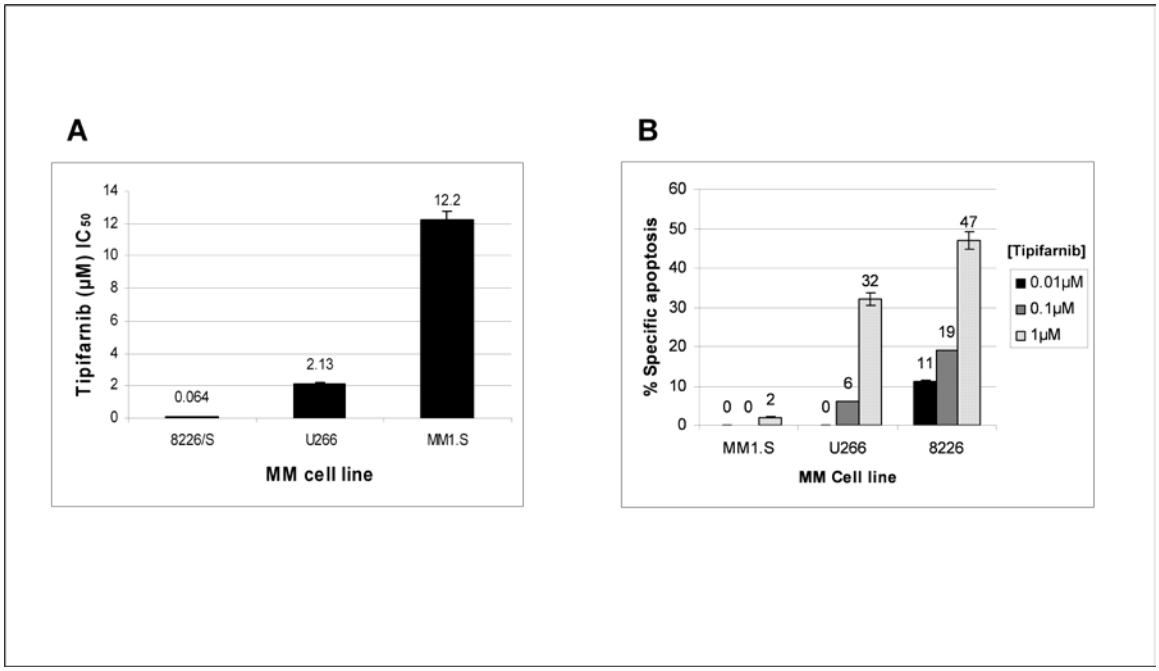

Figure 3.1. Myeloma cell lines show variable sensitivity to Tipifarnib *in vitro*. (A) Three myeloma cell lines were treated with log dilutions of Tipifarnib for 72 hours and viability measured by the MTT proliferation assay. Tipifarnib sensitivity was greatest in RPMI-8226 > U266 > MM1.S cells. (B) These cell lines were also treated either with vehicle control (DMSO), 10 nM, 100 nM, or 1 μM Tipifarnib for 48 hours. Cells were assayed for apoptosis using Annexin V-FITC/Propidium Iodide staining as determined by flow cytometry. To include early and late apoptotic events, values were derived as follows 100%-[(% viable of treated / % viable of DMSO ctrl /)100]. The same pattern of sensitivity as seen in the MTT assay can observed here. Data is presented as the avg of three independent experiments +/- SE.

3.3.2 Tipifarnib is cytotoxic to myeloma cell lines as exhibited in the SCID-hu model of disease

To investigate the effect of Tipifarnib on MM cell lines *in vivo*, we used a SCID-hu model of human myeloma previously described (URashima et al. 1997). SCID-hu mice had human fetal bone fragments implanted into their flanks and RPMI-8226 cells injected into the implant site. Urine immunoglobulin levels (M-Spike) were used to detect the establishment of disease in the mice. Mice were treated for 2 weeks with

Tipifarnib and sacrificed. The implanted bone tissue was removed and lymphocytes identified by Wright-Gimsa staining.

Urine λ-light chain levels in the untreated mice nearly doubled from 38.7 to 73.6 mg/L during the four week Tipifarnib treatment (Fig 3.3A). In contRast the λ-light chain levels in Tipifarnib treated mice were reduced from 28.6 mg/L to undetectable levels. The samples from mice receiving Tipifarnib treatment had significantly fewer myeloma cells compared to the control samples. Femur cross sections from a control animal display a bone with extensive disease (Fig 3.3B). In contRast, the sections from the Tipifarnib treated mice exhibited myloma cells to be located on the periphery of the sections in close proximity to the bone marrow stroma.

3.3.3 pAkt expression levels correlate with Tipifarnib cytotoxicity and drug resistance.

To determine if there was a correlation between Tipifarnib sensitivity and pAkt levels we examined pAkt expression on Tipifarnib treated cell lines. The pAkt levels in the highly sensitive RPMI-8226 cell line were negligible while a dose dependent decrease in Akt phosphorylation was observed in U266 cells (Fig. 3.4A). In contRast, the highly resistant MM1.S cells consistently express high levels of pAkt and exhibit no dose dependent decrease in its expression.

To examine the relationship between Akt phosphorylation and Tipifarnib sensitivity in an isogenic model I utilized the Tipifarnib resistant cell line, 8226/R5. Western blot analysis showed a dose dependent increase in Caspase-3 cleavage in the

Tipifarnib sensitive parental line, but no Caspase-3 activation was observed in 8226/R5 cells (Fig 3.4B). Furthermore, much like MM1.S cells, 8226/R5 cells express significantly high levels of pAkt, both at baseline levels and under the treatment of increasing concentrations of Tipifarnib.

3.3.4 IHC reveals elevated levels of nuclear localized pAkt in Tipifarnib resistant cells.

Immunohistochemical staining can complement western blotting data when attempting to evaluate the cellular localization of proteins. It has been implied that the signal mediating AKT localization is conformation dependant or is dependent upon the

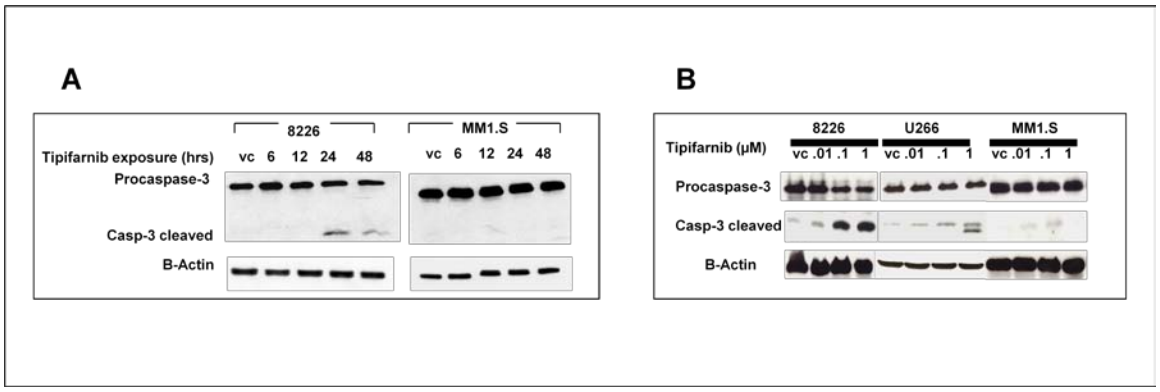

Fig 3.2 Drug sensitive Myeloma cell lines undergo Tipifarnib induced apoptosis as evidenced by Caspase-3 cleavage. (A) Time course experiment: 2 x 10^6 RPMI-8226 (8226) and MM1.S cell lines were simultaneously harvested after treatment with 1 μM Tipifarnib for the time-points indicated. Vehicle control (vc) samples were cells treated with DMSO for 48 hrs. Cell lysates were then immunoblotted for Procaspase and cleaved Caspase-3. The RPMI-8226 line showed evidence of Caspase-3 activation at 24 hours. While no Caspase activity was observed in MM1.S cells at the time points indicated. (b) Tipifarnib dose response assay: 2 x 10^6 RPMI-8226 (8226), U266 and MM1.S cells were treated with DMSO (vc), 10 nM, 100 nM, or 1 μM Tipifarnib for 48 hours. Cell lysates were then immunoblotted for Procaspase and cleaved Caspase-3. A dose dependent increase in Caspase-3 cleavage can be observed in 8226 and U266 cells however not in the highly Tipifarnib resistant MM1.S cell line.

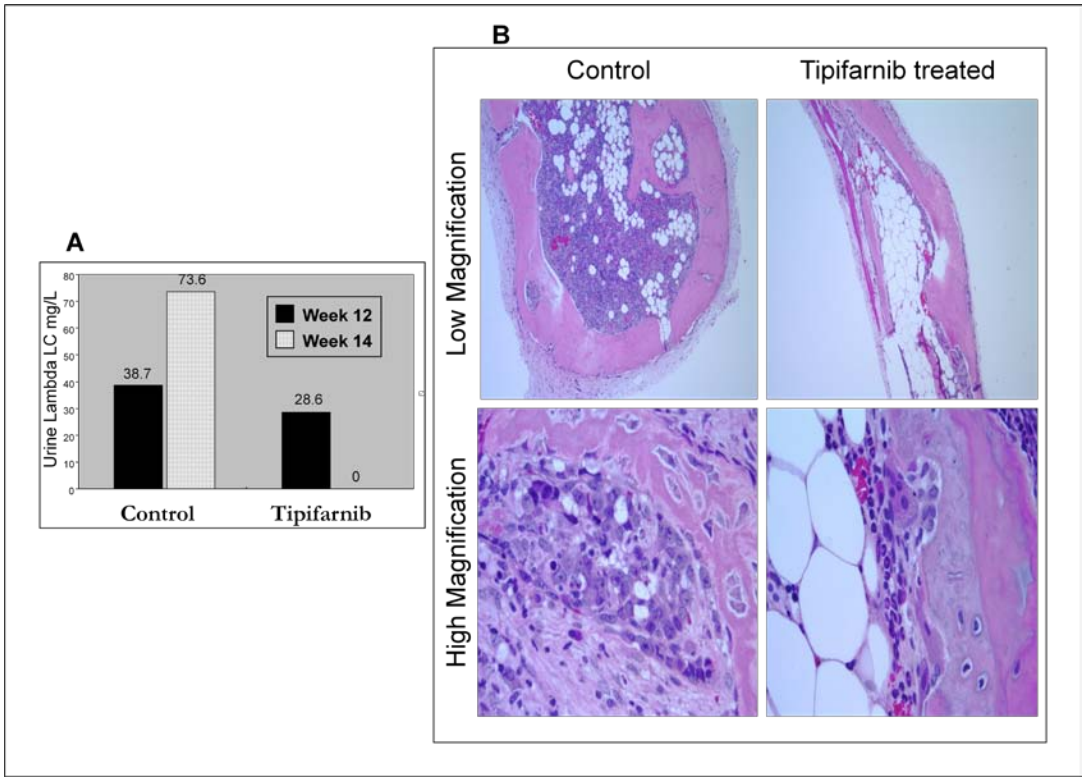

Figure 3.3 Tipifarnib is cytotoxic to RPMI-8226 cells in an *in vivo* murine model of multiple myeloma. Six to eight week old SCID mice were transplanted bilaterally, in the flanks with fetal human bone. Six weeks post-implant, human MM cells were injected into the implanted bones. Treatment commenced when the presence of disease was confirmed by ELISA detection of λ-light chain protein in the urine. (A) At 12 weeks post-implantation (week 12), before Tipifarnib treatment, both mice populations (control and Tipifarnib) showed significant levels of λ-light chain protein, 38.7 and 28.6 mg/L respectively in their urine. After 2 weeks of treatment with 50 mg/kg/d Tipifarnib (week 14), λ-light chain levels in control group mice nearly doubled to 73.6 mg/L while those in the Tipifarnib treated group were undetectable. (B) Following post-mortem removal and subsequent Wright-Gimsa staining of the implanted bones, histology exhibits a marked difference between the control and drug treated groups. Cross sections of bones from control mice show cavities nearly full of myeloma cells in the ctrl population. In contRast the Tipifarnib treated group show far less disease integration with most myeloma confined to the periphery of the marrow.

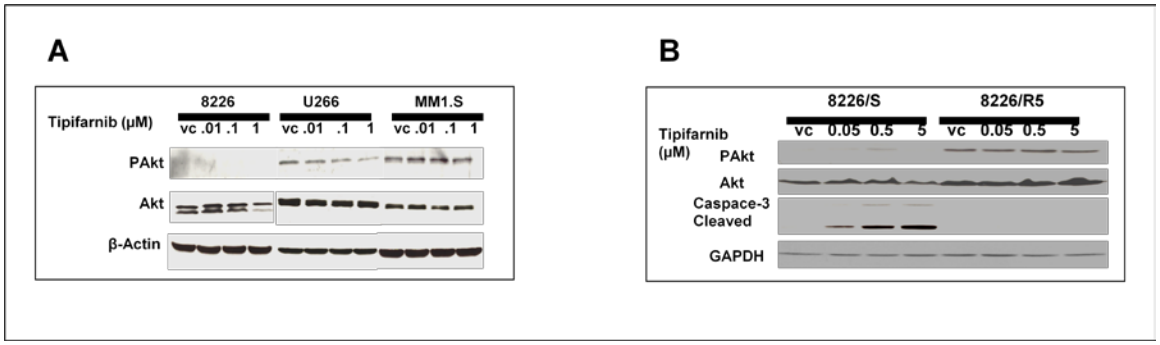

Figure 3.4 Tipifarnib dose response assay: 2 x 10^6 MM cells were treated with DMSO (vc), 10 nM, 100 nM, or 1 μM Tipifarnib for 48 hours. Cell lysates were then immunoblotted for Akt, pAkt(Ser473) or cleaved Caspase-3. (A) While endogenous Akt is expressed steadily across all three cell lines, the more resistant cell lines exhibit increased expression of activated Akt. pAkt expression in RPMI-8226 cells is not detectable by this method, whereas it is relatively highly expressed in the MM1.S cell line. Furthermore, we observed a dose dependent decrease in pAkt expression in U266 cells treated with Tipifarnib. (B) The RPMI-8226 Tipifarnib-resistant cell line (8226/R5) exhibits constitutive activation of Akt and increased endogenous levels of Akt as compared to the parental cells (8226/S). 8226/R5 cells, like MM1.S do not exhibit Caspase-3 activation with Tipifarnib treatment.

association with other proteins (Brattain et al. 2006). Because we and others believe Tipifarnib may be utilizing multiple pathways to induce apoptosis, we determined it possible that drug resistance to Tipifarnib may be not only associated with the hyperexpression of AKT but also its cellular localization. In this study, MM1.S and 8226/R5 cells expressing high levels of pAkt also exhibit a majority of the pAkt localized to the nucleus. This is exhibited by IHC utilizing the nuclear stain hematoxylin (Fig 3.5 A). Activated AKT is still not readily detectable in 8226/S cells using this method.

For further verification, nuclear and cytoplasmic extracts were prepared from 8226/S and 8226/R5 cells and probed with anti-pAkt and anti-Akt antibodies using anti-Poly ADP Ribose Polymerase (PARP) antibody as a control for the purity of the extracts

(Fig 3.5B). Even though 50µg of protein was evaluated in both nuclear and cytoplasmic extracts, the percentages of the target protein may be heavily increased. Thus, when evaluating AKT levels using a concentrated lysate such as obtained from a nuclear extract, pAkt is detectable in 8226/S cells, however pAkt and basal levels of AKT remain higher in the resistant cell line as made evident by consistent levels of the predominantly nuclear protein PARP between 8226/S and 8226/R5 nuclear extracts.

3.3.5 Ectopic expression of constitutively active AKT promotes cytotoxic resistance to Tipifarnib

Because of grave limitations with maintaining stable expression of exogenous proteins in 8226/S cells, the IL-3 dependant murine pro-B cells (Ba/F3) were used to ectopically express constitutively active AKT via the N-term addition of a myrostilation sequence which tethers Akt to the plasma membrane. Stable cell lines were created via selection in G418. This tethering increases its association with PI3K and phosphatidylinositol biphosphate rendering AKT constitutively active. Upon activation, AKT will release itself from the membrane and activate proteins such as MDM2, mTOR and NF-kB while inhibiting proteins such as BAD and FKHR. Membrane association exposes two crucial amino acids that are phosphorylated and necessary for activation.

Expression was confirmed by immunoblotting with AKT, pAkt and the cloned HA tag. The 30 kD shift noted between in dsRED-Myr-Akt and is accounted for by the

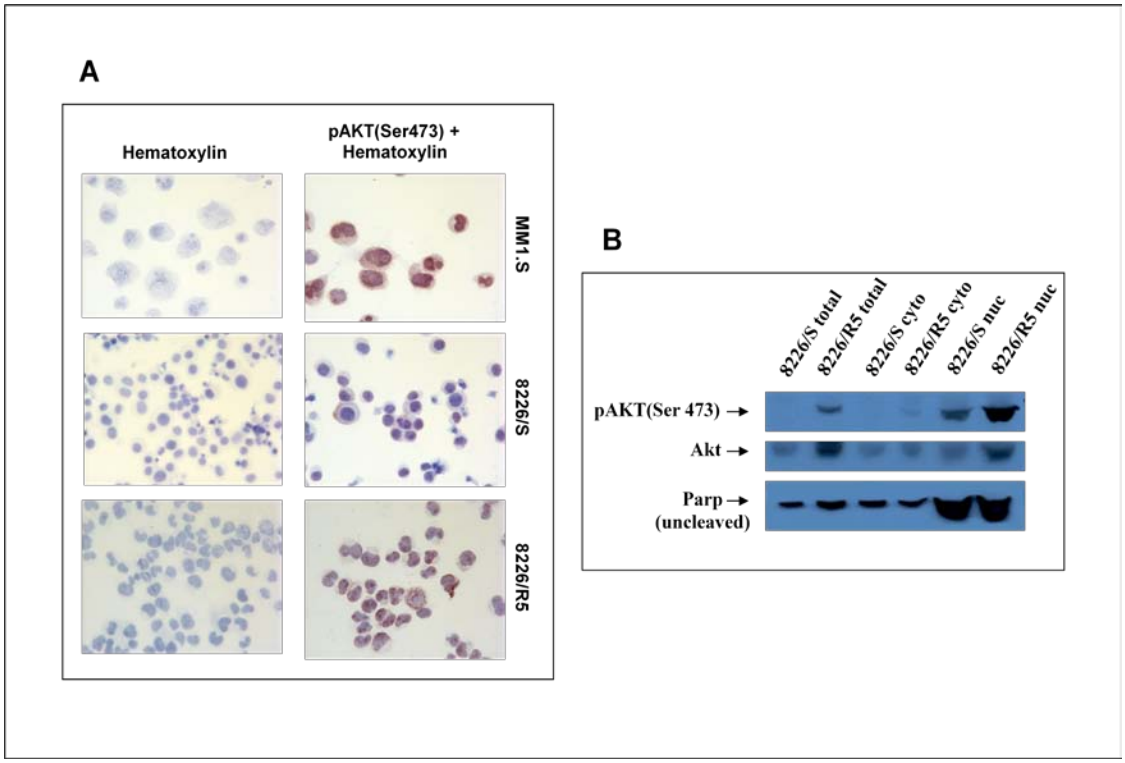

Figure 3.5 pAkt is nuclear localized in cells resistant to Tipifarnib. To perform IHC: 0.5 x 10^6 8226/S, 8226/R5 and MM1.S cells were cytospun fixed in 4 % paraformaldehyde and methanol methanol then incubated in saline plus pAkt(Ser473)-IHC Specific antibody. Slides were then washed in TBS, incubated with DAB reagent and stained with or without Hematoxylin. Cells were visualized by light microscopy and captures are representative of three independent experiments (A). Nuclear and cytoplasmic extracts were prepared from 8226/S and 8226/R5 cells. 50µg of cytoplasmic or nuclear protein was run on a 12% acrylamide gel and proteins were probed with antibodies for basal and activated AKT. Additionally uncleaved PARP expression was evaluated to asses the purity of the extracts.

fusion of the ~30 kD dsRED fluorescent protein (Fig 3.6 A). Importantly however, Ba/F3 cells exhibit a very similar sensitivity to Tipifarnib as RPMI-8226 cells (Fig 3.6 C) where 8226 (IC_{50}=114.348 nM) are only ~2.5-fold resistant to Tipifarnib compared with Ba/F3 cells (IC_{50}=40.562 nM).

Induction of Myr-Akt rendered Ba/F3 cells IL-3 independent as exhibited by Ba/F3(Myr-Akt) cells proliferating in the absence of IL-3. This transformed phenotype

has been seen with other well characterized tumor associated proteins including BCR-ABL, JAK1, JAK2 and STAT5 (Huang et al. 2005, Onishi et al. 1998, Daley et al. 1988) Addition of Ba/F3(Myr-Akt) conditioned medium to Ba/F3 cells did not support proliferation of the non-transformed cells. This suggests that Ba/F3(Myr-Akt) cells did not develop an autocrine growth factor loop capable of sustaining the cells in culture in the absence of IL-3 (data not shown).

Expression of pAkt in Ba/F3 cells rendered them to be ~57 fold resistant to Tipifarnib as compared to cells transfected with empty vector (Fig 3.6 C). Importantly, this fold resistance is similar to the phenotype held by 8226/S and 8226/R5 (~48 fold resistance).

Because of the presence of the *Discosoma sp.* red fluorescent protein in this construct, the localization of AKT could be evaluated and was found to be predominately nuclear in when stably expressed in this murine pro-B cell (Fig 3.6B).

3.4 Discussion

Understanding Tipifarnibs mechanism(s) of action is of significant importance. The drug has been shown to effectively induce apoptosis in both myeloma cell lines and primary isolates (Beaupre et al. 2003, Ochiai et al. 2003). *Alsina et al.* showed that 64% of patients experienced disease stabilization in a phase II clinical trial of patients with advanced multiple myeloma (Alsina et al. 2004). Tipifarnib did not receive Federal Drug Administration approval for the treatment of acute myeloid leukemia in 2005. Most

notably however the drug has exhibited extremely low toxicity in patients (Alsina et al. 2004) while we and others have postulated that Tipifarnib like other RAS inhibitors can be highly synergistic with a broad range of compounds including paclitaxel, tamoxifen

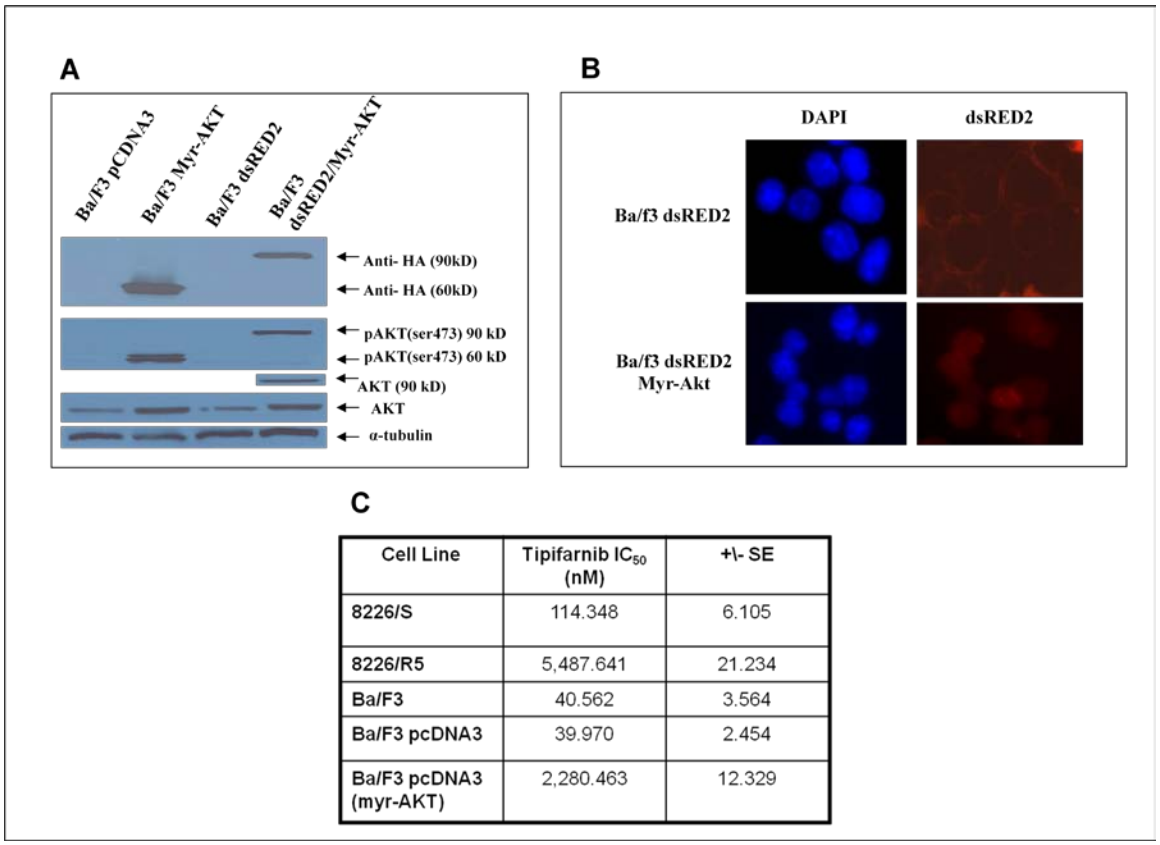

C

Cell Line	Tipifarnib IC_{50} (nM)	+\- SE
8226/S	114.348	6.105
8226/R5	5,487.641	21.234
Ba/F3	40.562	3.564
Ba/F3 pcDNA3	39.970	2.454
Ba/F3 pcDNA3 (myr-AKT)	2,280.463	12.329

Fig 3.6 Ectopic expression of constitutively active AKT promotes cytotoxic resistance to Tipifarnib. Ba/F3 cells stably expressing pDsRed2 and pDsRed2-HA-Myr-Akt1 were lysed and probed anti-HA, anti-pAkt and anti-Akt antibodies to verify expression. pAkt is only detectable in those cells transfected with the myrostilated engineered version of AKT (A).dsRED fluorescence was evaluated using DAPI staining to visualize the nucleus. Ba/F3 dsRED2 Myr-Akt cells exhibited dsRED fluorescence in the nucleus of cells (B). The MTT cytotoxity assay was utilized to determine the IC50 of Tipifarnib against Ba/F3 cells overexpressing active AKT. Ba/F3 cells exhibit a very similar sensitivity to Tipifarnib as RPMI-8226 cells (IC_{50}=114.348 nM) where 8226 (IC_{50}=114.348 nM) are only ~2.5-fold resistant to Tipifarnib compared with Ba/F3 cells (IC_{50}=40.562 nM). pAkt in Ba/F3 cells rendered them to be ~57 fold resistant to Tipifarnib as compared to cells transfected with empty vector (C). Data shown is representative of three independent experiments (A), 6 images taken on three separate days (B) or the average of 3 independent experiments +/- Standard Error (SE).

and Bortezomib among others (Lebowitz et al. 2005, Yanamandra et al. 2006, Zhu et al.). This suggests a promising future for FTIs in combination therapy.

Although FTIs were designed to obstruct Ras-prenylation, mounting evidence indicated that FTI induced cytotoxicity involves other pathways. FTI-SCH66336, FTI-277, and Perillic acid have all been suggested to function through non-Ras pathways including the NFκB, Akt2, and RhoA and Rac pathways (Takada et al. 2004, Jiang et al. 2000, Beaupre et al. 2003). Studies with Tipifarnib have likewise indicated that Ras-independent mechanisms may be involved. It has been reported that Tipifarnib cytotoxicity in neoplastically transformed mouse cells is RhoB dependent (DuHadaway et al. 2003). In human myeloma cell lines Tipifarnib has been suggested to induce apoptosis via other Ras-independent mechanisms, including the JAK/STAT pathway and/or through Bax activation of an ER stress response (Beaupre et al. 2004, Le Gouill et al. 2002).

Here we report a correlation between pAkt levels and sensitivity to Tipifarnib, where the cell lines expressing low or minimal levels of pAkt show to be relatively more sensitive than those cells with high levels of pAkt. These results are consistent with observations made by one group in a phase II clinical trial (Alsina et al. 2004). A variance in p-Akt expression was observed between all three myeloma lines tested. Furthermore, the variation in pAkt expression was even more pronounced between standard RPMI-8226/S cells and the Tipifarnib-resistant RPMI-8226/R5 cell line. Additionally, it has been reported that overexpressed constitutively active myr-Akt can

overcome the pro-apoptotic effects of FTI (Du et al. 1999). These findings indicate Akt may be an excellent target for combination drug therapy.

Chapter 4

Tipifarnib and Bortezomib Are Synergistic and Overcome Cell Adhesion–Mediated Drug Resistance in Multiple Myeloma and Acute Myeloid Leukemia

Chapter 4 represents the following publication: Yanamandra et al. 2006

4.1 Introduction

It has been established in preclinical models of multiple myeloma and acute myeloid leukemia (AML) that the bone marrow microenvironment provides protection from chemotherapy- and death receptor–mediated apoptosis. This form of resistance, termed *de novo* drug resistance, occurs independent of chronic exposure to cancer-related therapies and likely promotes the development of multidrug resistance. Consequently, it is of major interest to identify compounds or drug combinations that can overcome environment-mediated resistance. In this study, we investigated the activity of Tipifarnib (Zarnestra, formerly R115777) combined with Bortezomib (Velcade, formerly PS-341) in microenvironment models of multiple myeloma and AML. The combination proved to be synergistic in multiple myeloma and AML cell lines treated in suspension culture. Even in tumor cells relatively resistant to Tipifarnib, combined activity was maintained. Tipifarnib and Bortezomib were also effective when multiple myeloma and AML cells

were adhered to fibronectin, providing evidence that the combination overcomes cell adhesion–mediated drug resistance (CAM-DR). Of importance, activation of the endoplasmic reticulum stress response was enhanced and correlated with apoptosis and reversal of CAM-DR. Multiple myeloma and AML cells cocultured with bone marrow stromal cells also remained sensitive, although stromal-adhered tumor cells were partially protected (relative to cells in suspension or fibronectin adhered). Evaluation of the combination using a transwell apparatus revealed that stromal cells produce a protective soluble factor. Investigations are under way to identify the cytokines and/or growth factors involved. In summary, our study provides the preclinical rationale for trials testing the Tipifarnib and Bortezomib combination in patients with multiple myeloma and AML.

Multiple myeloma and acute myeloid leukemia (AML) are cancers with high mortality rates, where novel strategies are required to improve on current treatment standards. It has been well established in multiple myeloma and other malignancies that the interaction between tumor cells and elements of their microenvironment results in resistance to chemotherapy- and death receptor–mediated apoptosis (Hazlehurst et al. 2003). This form of resistance, termed *de novo* drug resistance, occurs independent of chronic exposure to chemotherapy and likely promotes the development of multidrug resistance (Shain et al. 2001).

Two basic components comprise environment-mediated drug resistance: physical contact between tumor cells and microenvironment components (cell adhesion mediated drug resistance, CAM-DR) and the local production of soluble factors. More specifically, in multiple myeloma and AML, it has been found that the adhesion of tumor cells (via

integrin receptors) to fibronectin results in a drug-resistant phenotype (Hazlehurst et al. 2003, Matsunaga et al. 2003). Of importance, in a small series of AML patients, it was noted that those whose leukemic cells expressed VLA-4 ($\alpha_4ß_1$ integrin) had a high rate of relapse compared with those with low VLA-4 expression (Matsunaga et al. 2003). These results imply that the physical interaction between tumor cells and bone marrow constituents provides a refuge for minimal residual disease. Tumor-microenvironment contact also results in the production of soluble factors that can further accentuate the drug resistant phenotype (Nefedova et al. 2003). In multiple myeloma and AML, cytokines, such as interleukin-6 (IL-6), IL-1ß, and vascular endothelial growth factor, have been implicated as important growth and survival factors, and these molecules may also contribute to environment-mediated resistance. Based on the knowledge that the mechanisms of *de novo* drug resistance are unique and genetically distinct from those associated with acquired resistance (Hazlehurst et al. 2003), it is of major interest to identify compounds or drug combinations that are specifically active on tumor cells protected by the microenvironment compartment.

The proteasome inhibitor Bortezomib (Velcade, formerly PS-341) has been found to have clinical activity in patients with relapsed multiple myeloma (Kane et al. 2003). Bortezomib is a reversible inhibitor of the 26S proteasome, a complex that plays a major role in protein degradation. Inhibition of this complex ultimately leads to inactivation of the transcription factor nuclear factor-κB, a survival protein that is thought to be one of the drugs main targets. A previous study has reported that Bortezomib can reverse the CAM-DR phenotype in a multiple myeloma cell line (Mitsiades et al. Blood 2003).

Interestingly, we made similar observations testing the compound Tipifarnib (Zarnestra, formerly R115777) in multiple myeloma and AML cells. Tipifarnib is a farnesyl transfeRase inhibitor (FTI) that inhibits the membrane localization of Ras resulting in a loss of function (End et al. 2001). Tipifarnib has been clinically tested in patients with multiple myeloma and AML and was found to be active in both diseases (Alsina et al. 2004, Karp et al. 2001). In this study, we investigate the combination of Tipifarnib and Bortezomib in microenvironment models of multiple myeloma and AML. Our data provide preclinical evidence of activity for this novel drug combination.

4.2 Materials and Methods

4.2.1 Cell Lines

RPMI 8226/S, H929, U266, KG-1, and U937 lines were obtained from the American Type Culture Collection (Manassas, VA). MM1s cells were kindly provided by Steven Rosen (Northwestern University, Chicago, IL). 8226/S, U266, U937, and MM1s cells were maintained in RPMI 1640 supplemented with 100 mmol/L l-glutamine (Mediatech, Inc., Herndon, VA) and 10% fetal bovine serum (FBS; Omega Scientific, Inc., Tarzana, CA). H929 cells were maintained in RPMI 1640 supplemented with 10% FBS and 0.05 mol/L 2-mercaptoethanol (Sigma Chemical, St. Louis, MO). The KG-1 line was maintained in Iscove's modification of DMEM (Mediatech) with 4 mmol/L L-glutamine, 25 mmol/L HEPES, and 20% FBS. HS-5 bone marrow stromal cells were

obtained from the American Type Culture Collection and maintained in RPMI 1640 supplemented with 100 mmol/L L-glutamine, 10% FBS, and 1% penicillin/streptomycin. HS-5 green fluorescent protein (GFP) stromal cells were developed by stably expressing enhanced green fluorescent protein under hygromycin (Invitrogen, Carlsbad, CA) selection (50 μg/mL).

4.2.2.Compounds

Tipifarnib was kindly provided by David End (Johnson & Johnson Pharmaceutical Research and Development, LLC, Titusville, NJ). Tipifarnib was dissolved in 100% DMSO (Sigma Chemical) and sonicated for 10 minutes at room temperature. Bortezomib (Millennium Pharmaceuticals, Cambridge, MA) was also dissolved in 100% DMSO, and both compounds were stored at –20°C before use.

4.2.3 Patient samples.

Multiple myeloma and AML patient samples were collected under two Institutional Review Board–approved protocols (MCC# 13715 and MCC# 13947/13355). After obtaining informed consent for bone marrow aspiration, mononuclear cells were isolated by Ficoll-Hypaque gradient purification as per the manufacturer's instructions (Amersham Biosciences, Piscataway, NJ). Primary isolates were exposed to Tipifarnib and Bortezomib and analyzed as described below.

To establish patient bone marrow stromal cells, multiple myeloma patient specimens with <20% myeloma cells were cultured continuously in MEM-α medium (Invitrogen) supplemented with 15% FBS and 1% penicillin with streptomycin until an adherent layer of stromal cells predominated. AML patient specimens were processed by $CD33^+$ selection using CD33 microbeads and the AutoMacs magnetic cell sorter (Miltenyi Biotec, Inc., Auburn, CA). $CD33^-$ populations were cultured continuously as above. For coculture experiments, stromal cells were seeded to near confluence and incubated overnight at 37°C. Cell lines were adhered, exposed to Tipifarnib and Bortezomib, and analyzed as described below.

4.2.4 Combination index analysis.

The dose-effect relationship between Tipifarnib and Bortezomib was analyzed using CalcuSyn software (Biosoft, Ferguson, MO). The combination index equation is based on the following multiple drug effect equation of Chou-Talalay (Chou et al. 1984): combination index = $(D)_1 / (D_x)_1 + (D)_2 / (D_x)_2 + (D)_1(D)_2 / (D_x)_1 / (D_x)_2$. Combination index = 1, >1, or <1 is considered additive, antagonistic, or synergistic, respectively. Drug combination studies were based on the fraction of cells affected relative to untreated controls. The mean and SD of the combination index were calculated using the Monte Carlo algorithm. To evaluate the relative contribution of each agent, 8226 and U937 cells were seeded at 1×10^3 per well and exposed to five concentrations of Tipifarnib, Bortezomib, and the combination (constant molar ratio, 100:1). After 72 hours at 37°C,

cytotoxicity was measured by 3-(4,5-dimethylthiazol-2-yl)-2,5-diphenyltetrazolium bromide assay as previously described (Damiano et al. 1999).

4.2.5 Fibronectin adhesion and cell death analysis.

Adhesion of primary isolates and tumor cell lines to fibronectin was done as previously described (Damiano et al. 1999). For cell lines, adhered tumor cells were incubated overnight at 37°C, and then control-supplemented media or Bortezomib ± Tipifarnib was added for an additional 24 hours. In primary isolates, control-supplemented media or Bortezomib ± Tipifarnib was added for 24 hours after 2 hours of adhesion. In parallel, primary isolates or tumor cell lines were cultured in 0.1% bovine serum albumin–coated plates (Boehringer-Mannheim, Indianapolis, IN; multiple myeloma) or 0.1% poly-hema (Sigma, St. Louis, MO)–coated plates (AML) and exposed to control media or Bortezomib ± Tipifarnib as above. Cell death was determined by flow cytometry after Annexin V/FITC (Biovision, Mountain View, CA) and propidium iodide (Biovision) or 7-amino actinomycin-D (BD PharMingen, San Jose, CA) staining as described previously (Beaupre et al. 2003). In primary isolates, samples were also stained with anti CD138 (BD PharMingen, San Jose, CA; myeloma cells) or anti CD33 (BD PharMingen; leukemic cells) antibodies to identify tumor cell populations.

4.2.6 Adhesion assays.

Adhesion assays were done similar to previously described (Damiano et al. 1999) using the cell tracker 5-chloromethylfluorescein diacetate (Molecular Probes, Eugene, OR). For pre-adhesion drug treatment, tumor cells were incubated with Tipifarnib (5 μmol/L), Bortezomib (5 nmol/L), or the combination for 2 hours before adhesion to fibronectin. After 2 hours of adhesion, wells were washed and fluorescence was measured at 490 nm on a Wallac Victor-2 1420 Multilabel Counter. For post-adhesion drug treatment, tumor cells were stained with 5-chloromethylfluorescein diacetate (as above) and then adhered to fibronectin for 2 hours followed by exposure to Tipifarnib (5 μmol/L), Bortezomib (5 nmol/L), or the combination for an additional 2 hours. Wells were then washed, and absorbance was read as described.

4.2.7 Adhesion to bone marrow stroma and cell death analysis

In coculture experiments, HS-5 GFP stromal cells were seeded to near confluence and incubated overnight at 37°C. The next morning, stromal cells were washed once with serum-free medium, and primary isolates or tumor cell lines were allowed to adhere for 2 hours in either serum-free MEM (Alpha MEM, Invitrogen) or RPMI 1640, respectively. Nonadhered cells were removed, and samples were then exposed to control supplemented media or Bortezomib ± Tipifarnib for 24 to 36 hours (see figure legends). Percent cell death was determined by flow cytometry as described above. For coculture experiments

involving cell lines, gating on GFP^- populations identified tumor cells. In primary isolates, additional staining with anti-CD138 (myeloma cells) or anti-CD33 (leukemic cells) antibodies distinguished tumor cells from background mononuclear cells. For our experiments, we also determined the number of live cells per sample using flow cytometry as previously described (Beaupre et al. 2003).

4.2.8 Transwell analysis

8226 myeloma and U937 leukemia cells were either adhered (as described above) or separated from HS-5 GFP stromal cells by a Transwell insert (costar, 0.4-µm mesh, 12-mm diameter; Corning, Corning, NY). Cells were treated with either control-supplemented media or the Tipifarnib (5 µmol/L) and Bortezomib (5 nmol/L) combination for 36 hours. Cell death was determined by flow cytometry after staining with Annexin V/FITC and 7-amino actinomycin-D. Cell death of multiple myeloma and AML cells was determined in coculture by gating on GFP^- populations.

4.2.9 Western blotting

Western blotting was done as described previously (Beaupre et al. 2003) . Antibodies were purchased from the following vendors: GADD153 and anti-K-Ras-2B (Santa Cruz Biotechnology, Santa Cruz, CA), ß-actin (Sigma Chemical), anti-HDJ-2 (NeoMarkers, Freemont, CA). Densitometry was done by scanning radiographic images,

and bands were quantitated using Alpha Ease image analysis software (Alpha Innotech Corp., San Leandro, CA).

4.2.10 Proteasome assay

8226/S myeloma cells (4×10^6) were exposed to control media, Tipifarnib, Bortezomib, or the combination for 2 hours at 37°C. Cells were harvested, washed twice with ice-cold PBS, and then lysed in 50 µL of TE buffer [10 mmol/L Tris, 1 mmol/L EDTA (pH 7.9)]. Total protein was quantitated using a Bio-Rad protein assay kit (Hercules, CA), and 10 µg of protein were analyzed for proteasome activity using a 20S proteasome activity assay as per the manufacturer's instructions (Chemicon International, Temecula, CA).

4.3 Results

4.3.1 Tipifarnib and Bortezomib are synergistic in multiple myeloma and AML cell lines.

It has previously been reported that FTIs and proteasome inhibitors induce apoptosis in multiple myeloma (Mitsiades et al. 2003, Beaupre et al. 2003, Le Gouill et al. 2002, Bolick et al. 2003, Hideshima et al. 2001) and leukemic (Beaupre et al. 1999, Dai et al. 2003) (cell lines. By analyzing the activity of Tipifarnib and Bortezomib as single agents in several representative lines, we defined concentrations with low toxicity

for combination studies (data not shown). We first tested Tipifarnib and Bortezomib on a diverse group of myeloma lines maintained in suspension culture (Fig 4.1 A-C). Evidence for greater than additive cell death was observed and was most pronounced in H929 and MM1s cells (Fig 4.1 A and C). Interestingly, the MM1s line was relatively resistant to single-agent Tipifarnib, yet the combination maintained its activity. We also tested KG-1 leukemia cells and found that they were sensitive although to a lesser degree when compared with our myeloma lines (Fig 4.1D). To confirm that Tipifarnib and Bortezomib were synergistic in vitro, 8226/S myeloma cells and U937 leukemia cells were treated with single-agent Tipifarnib, Bortezomib, and the combination in cell suspension.
Combination index analysis revealed synergistic activity between the two compounds at several dose combinations tested (Fig 4.2 A and B). These results indicate that Tipifarnib combined with Bortezomib is an active regimen in diverse multiple myeloma and AML cell lines.

4.3.2 Tipifarnib combined with Bortezomib overcomes CAM-DR.

It has previously been established that adherence of multiple myeloma and AML cells to the extracellular matrix component fibronectin results in resistance to chemotherapeutic agents, including melphalan, doxorubicin, and cytosine arabinoside (Matsunaga et al. 2003). To determine whether Tipifarnib and Bortezomib overcome CAM-DR, 8226/S myeloma (Fig 4.3A and B) and U937 leukemia cells (Fig 4.3 C and D) were adhered

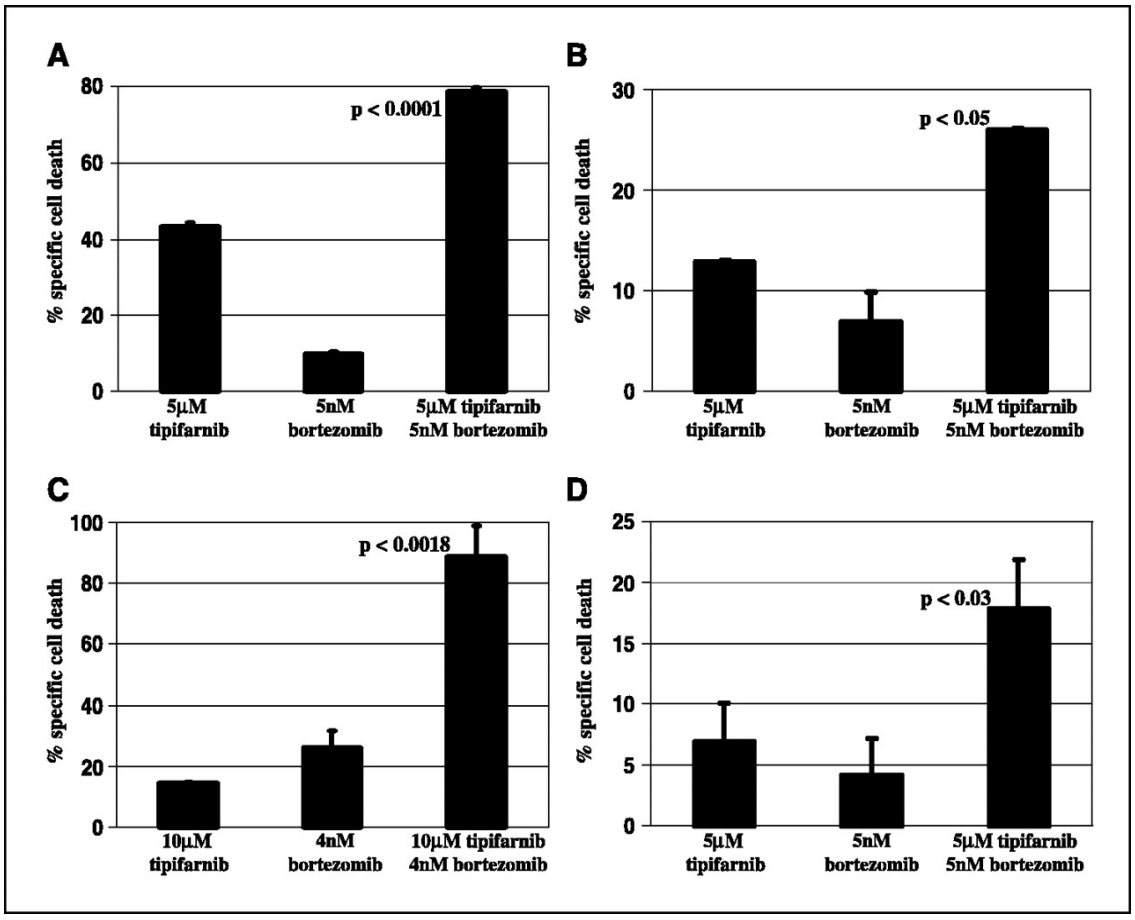

Fig. 4.1 Tipifarnib combined with Bortezomib induces cell death in diverse multiple myeloma and AML cell lines. H929 (*A*), U266 (*B*), MM1s (*C*), or KG-1 (*D*) cell lines were treated with the indicated concentrations of Tipifarnib, Bortezomib, or the combination for 24 hours in cell suspension. Cell death was determined by flow cytometry after Annexin V/FITC and propidium iodide staining. Specific cell death was calculated relative to untreated controls. Three independent experiments. To identify evidence for greater than additive effect, a simple linear regression (no intercept model) was used that included drug effect for each individual drug and the interaction effect of the combination. SAS software was used in the calculations using Proc REG (n = 9 observations for each cell line). *P*s are provided. Columns, mean; bars, SE.

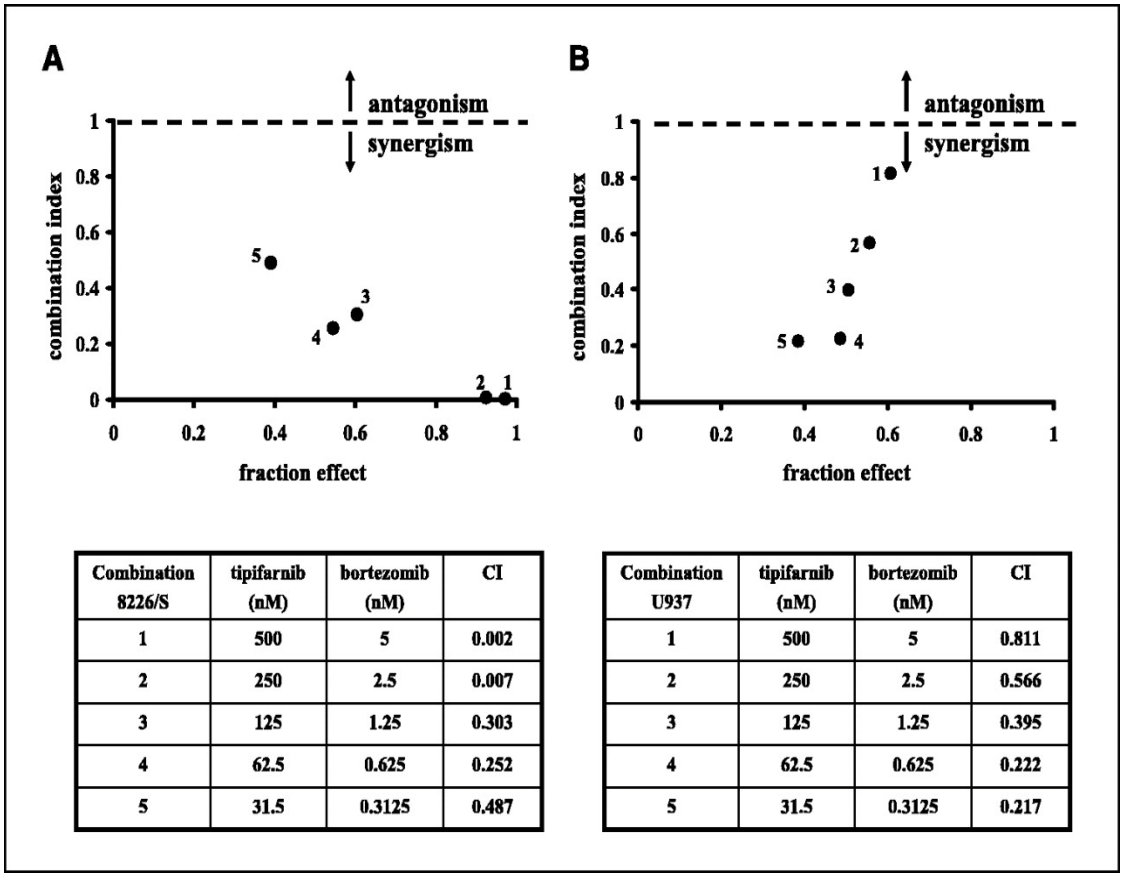

Combination 8226/S	tipifarnib (nM)	bortezomib (nM)	CI
1	500	5	0.002
2	250	2.5	0.007
3	125	1.25	0.303
4	62.5	0.625	0.252
5	31.5	0.3125	0.487

Combination U937	tipifarnib (nM)	bortezomib (nM)	CI
1	500	5	0.811
2	250	2.5	0.566
3	125	1.25	0.395
4	62.5	0.625	0.222
5	31.5	0.3125	0.217

Fig. 4.2 Tipifarnib and Bortezomib are synergistic in cytotoxicity assays. 8226/S (*A*) and U937 (*B*) cells were treated with Tipifarnib, Bortezomib, or a constant molar ratio (100:1) of the combination for 72 hours. Cytotoxicity was determined using 3-(4,5-dimethylthiazol-2-yl)-2,5-diphenyltetrazolium bromide assays (as described in Materials and Methods). The resulting data was used to generate combination index plots (*CI*) for various dose combinations. The dashed line indicates additive affect (CI = 1). Antagonism (*above dashed line*) and synergism (*below dashed line*). Tables are included to provide the drug concentrations tested. Points, average of quadruplicate values of three independent experiments; bars, SD.

to fibronectin and evaluated for sensitivity to single-agent Tipifarnib and Bortezomib. In both lines and with both compounds, a dose-dependent increase in cell death was observed in suspension and fibronectin-adhered tumor cells. Importantly, fibronectin adherence did not protect tumor cells from Tipifarnib- or Bortezomib-induced apoptosis. Furthermore, the Tipifarnib and Bortezomib combination consistently induced cell death more efficiently in adhered 8226/S and U937 cells when compared with cells treated in

suspension (Fig 4.3 E). Evaluation of three multiple myeloma and five AML patient samples also revealed that fibronectin-adhered primary tumor isolates were not protected (Fig 4.3E). These results indicate that Tipifarnib combined with Bortezomib overcomes the CAM-DR phenotype.

4.3.3 Reversal of CAM-DR is not related to decreased tumor adherence.

Because it has been reported that Bortezomib can alter the expression of adhesion molecules (Read et al. 1995), we addressed whether the activity of Tipifarnib and Bortezomib was related to decreased adherence of tumor cells to fibronectin. 8226/S myeloma cells (Fig 4.4 A) and U937 leukemia cells (Fig 4.4 C) were exposed to Tipifarnib, Bortezomib, or the combination for 2 hours before adhesion to fibronectin. Tumor cell attachment was not prevented in either line, and pre-adhesion drug exposure for up to 8 hours revealed no significant decrease in attachment relative to controls (data not shown). To verify that Tipifarnib and Bortezomib did not reverse cell adhesion in attached tumor cells, 8226/S (Fig 4.4 B) and U937 (Fig 4.4 D) cells were exposed to Tipifarnib, Bortezomib, or the combination for 2 hours after being adhered to fibronectin. Once again, we detected no reduction in tumor cell adhesion that could explain sensitivity to the Tipifarnib and Bortezomib combination.

4.3.4 Activation of endoplasmic reticulum stress correlates with reversal of CAM-DR.

It has been reported that the antitumor activity of isoprenoid inhibitors (such as FTIs and geranylgeranyl transfeRase inhibitors) may in part be related to inhibition of the proteasome proteolytic pathway. We therefore evaluated proteasome proteolysis in tumor cells after Tipifarnib and Bortezomib treatment. We found that Tipifarnib had little to no effect on endogenous proteasome activity, and the combination was no more active than Bortezomib alone (Fig 4.5 A). Similarly, inhibition of FTase (using HDJ-2 prenylation as a surrogate marker) was also not enhanced (Fig 4.5 B). Inhibition of K-Ras farnesylation was not observed after treatment with Tipifarnib and/or Bortezomib, consistent with our prior report of a Ras-independent mechanism of cell death (Beaupre et al. 2004). These results indicate that enhanced activity at the purported targets of Tipifarnib and Bortezomib is not responsible for drug synergy; rather, events downstream of the 26S proteosome and FTase likely cooperate to activate intrinsic proapoptotic cascades.

It has been shown that proteasome inhibitors induce apoptosis in myeloma cells via triggering of endoplasmic reticulum (ER) stress with subsequent disruption of the unfolded protein response (Lee et al. 2003). It has also been observed that proteasome inhibitors combined with other compounds that activate ER stress (such as tunicamycin) induce cell death in synergy (Lee et al. 2003). Of relevance, we found that Tipifarnib activates the ER stress response in multiple myeloma cell lines (Beaupre et al. 2004). Based on these observations, we surmised that apoptosis induced by Tipifarnib and Bortezomib may be related to activation of the ER stress response. Therefore, 8226/S

myeloma cells were exposed to Tipifarnib, Bortezomib, or the combination for 24 hours either in suspension culture or after being adhered to fibronectin (Fig 4.5 C). Activation of ER stress was determined by monitoring the expression of GADD153, a well-established ER stress marker (Wang et al. 1996). We found that both Tipifarnib and Bortezomib increased GADD153 expression under suspension and adhered conditions consistent with their ability to activate ER stress–related cascades. Importantly, the combination enhanced the ER stress response particularly under fibronectin-adhered conditions. These results imply a link between reversal of CAM-DR and activation of the ER stress response.

4.3.5 Stroma-adhered tumor cells are sensitive to Tipifarnib and Bortezomib.

Due to the fact that soluble factors may also participate in environment-mediated drug resistance, we tested Tipifarnib and Bortezomib in coculture models of the bone marrow microenvironment. 8226/S myeloma cells were adhered to HS-5 bone marrow stromal cells and then exposed to increasing concentrations of Bortezomib (Fig 4.6 A) or Tipifarnib (Fig 4.6 B) for 24 hours. The percentage of live cells decreased in a dose-dependent manner after treatment with both compounds, and importantly, stroma-adhered 8226/S cells were nearly as sensitive as suspension cells. Also of significance was the fact that high concentrations of Bortezomib and Tipifarnib were not cytotoxic to cocultured HS-5 stromal cells (Fig 4.6 A and B). Combined activity was maintained in both stroma-

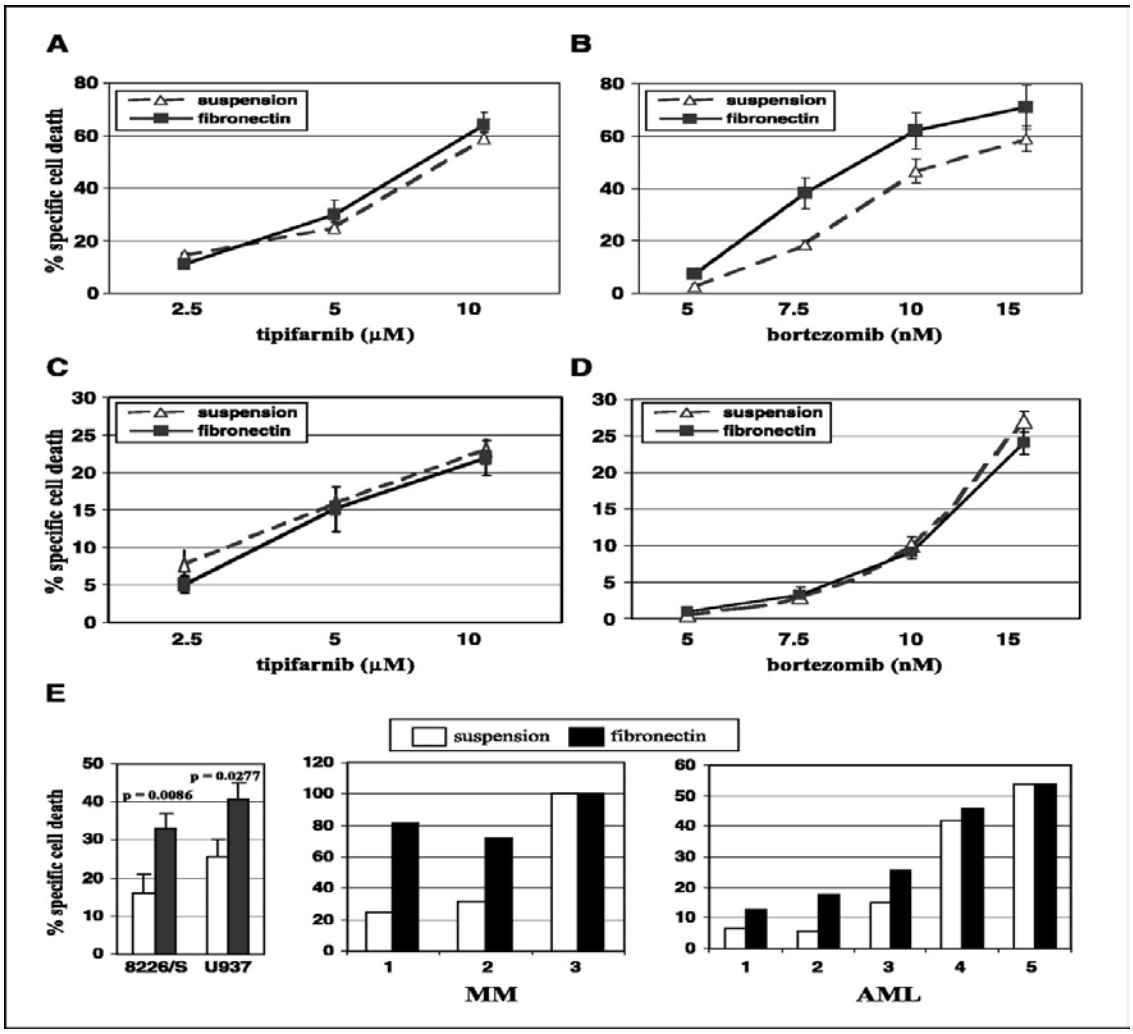

Fig. 4.3. Tipifarnib and Bortezomib induce cell death in fibronectin adhered multiple myeloma (*MM*) and AML cells. 8226/S myeloma cells (*A* and *B*) and U937 leukemic cells (*C* and *D*) were treated with the indicated concentrations of Tipifarnib or Bortezomib for 24 hours either in cell suspension or after adhesion to fibronectin. Cell death was determined by flow cytometry after Annexin V/FITC and propidium iodide staining. Combined from three independent experiments (*A-D*). *E*, 8226/S and U937 cell lines along with mononuclear cells from three multiple myeloma and five AML patients were exposed to 5 μmol/L Tipifarnib and 5 nmol/L Bortezomib for 24 hours either in cell suspension or after adhesion to fibronectin. Cell death was determined as in (*A-D*). In primary isolates, tumor cells were identified by staining with anti-CD138 (myeloma cells) or anti-CD33 (leukemic cells) antibodies. For cell lines, five (8226/S) and seven (U937) independent experiments were compared using a paired *t* test with *P*s. Columns/points, mean; bars, SE.

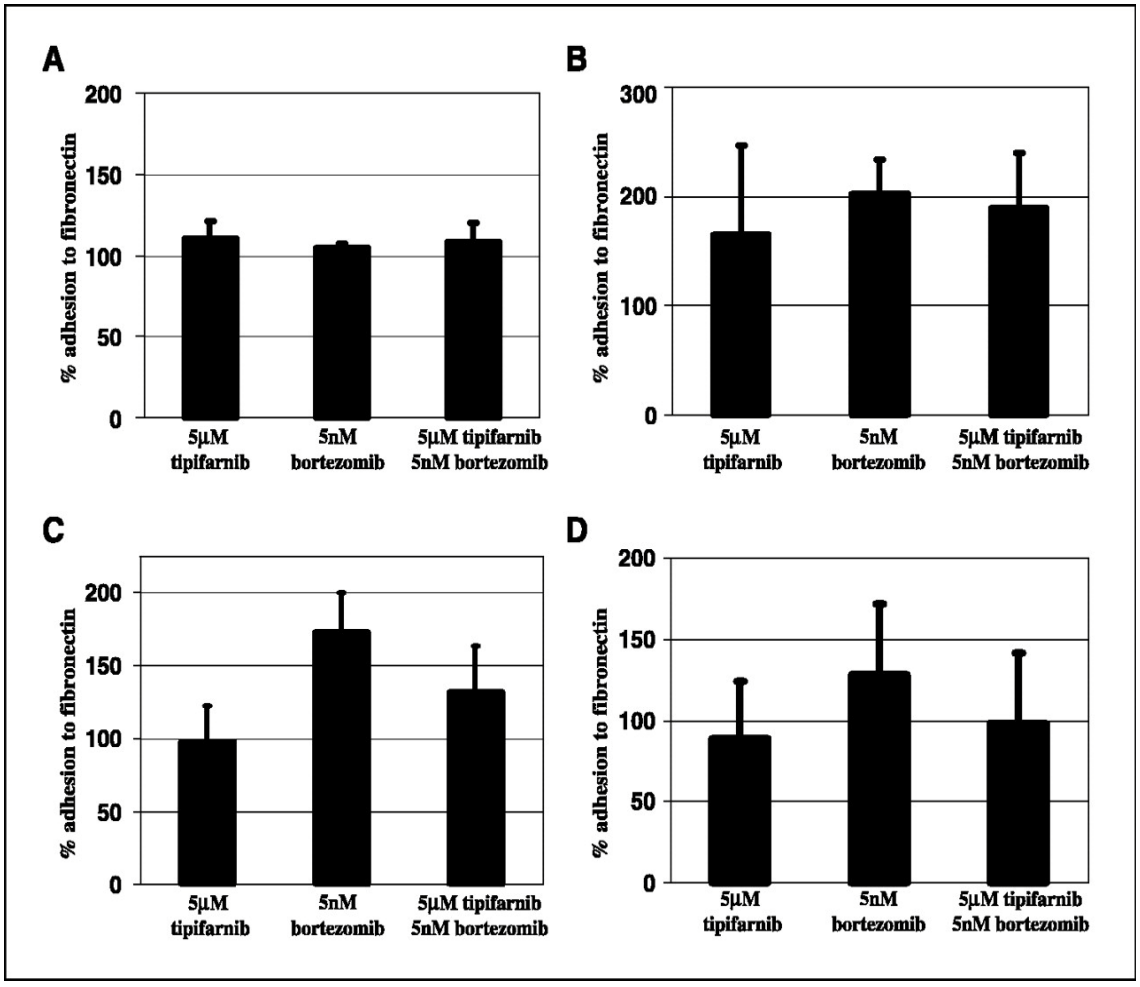

Fig. 4.4 Adhesion to fibronectin is not disrupted by Tipifarnib and Bortezomib. 8226/S myeloma cells (*A* and *B*) and U937 leukemic cells (*C* and *D*) were stained for 30 minutes with the cell tracker 5-chloromethylfluorescein diacetate (see Materials and Methods). *A* and *C*, cells were washed and then treated with the indicated concentrations of Tipifarnib, Bortezomib, or the combination for 2 hours (pre-adhesion exposure). After drug treatment, cells were adhered to fibronectin for an additional 2 hours and washed, and fluorescence was analyzed on a fluorescence plate reader. *B* and *D*, cells were adhered to fibronectin for 2 hours and then exposed to the indicated concentrations of Tipifarnib, Bortezomib, or the combination for an additional 2 hours (post-adhesion exposure). Samples were washed, and fluorescence was measured as in (*C* and *D*). Combined from three independent experiments. Percent adhesion to fibronectin is relative to cells treated with control media only. Columns, mean; bars, SE.

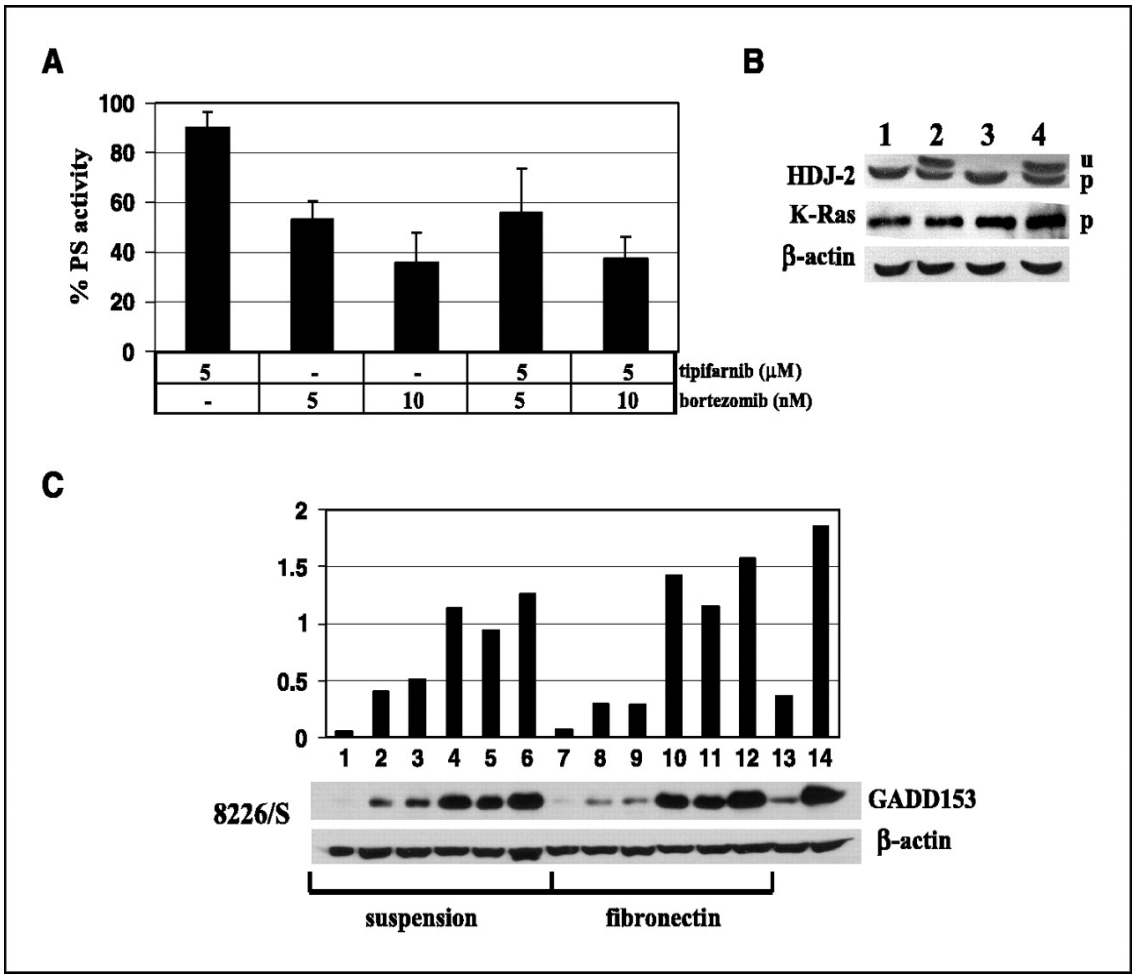

Fig. 4.5 Reversal of CAM-DR correlates with activation of the ER stress response. *A*, 8226 myeloma cells were treated with the indicated concentrations of Tipifarnib and Bortezomib in cell suspension for 2 hours. Proteasome activity was measured as described in Materials and Methods. Percent proteasome (*PS*) activity is relative to cells treated with control media. *B*, 8226/S myeloma cells were treated with control media (*lane 1*), 5 μmol/L Tipifarnib (*lane 2*), 5 nmol/L Bortezomib (*lane 3*), or the combination (*lane 4*) for 24 hours in cell suspension. Cell lysates were harvested and analyzed by Western blotting using the indicated antibodies. u, unprocessed HDJ-2; p, processed HDJ-2 or K-Ras. *C*, 8226 myeloma cells were treated for 12 hours in cell suspension or after adherence to fibronectin as follows: suspension, control media (*lane 1*), 5 μmol/L Tipifarnib (*lane 2*), 5 nmol/L Bortezomib (*lane 3*), 10 nmol/L Bortezomib (*lane 4*), 5 μmol/L Tipifarnib and 5 nmol/L Bortezomib (*lane 5*), 5 μmol/L Tipifarnib and 10 nmol/L Bortezomib (*lane 6*); fibronectin, control media (*lane 7*), 5 μmol/L Tipifarnib (*lane 8*), 5 nmol/L Bortezomib (*lane 9*), 10 nmol/L Bortezomib (*lane 10*), 5 μmol/L Tipifarnib and 5 nmol/L Bortezomib (*lane 11*), 5 μmol/L Tipifarnib and 10 nmol/L Bortezomib (*lane 12*). As a control for ER stress, U266 cells were either treated with control media (*lane 13*) or 25 μmol/L tunicamycin (*lane 14*) for 12 hours. Cell lysates were harvested and analyzed by Western blotting using the indicated antibodies. Densitometric evaluation of bands. *A*, combined from three independent experiments. *B* and *C*, representative of two independent experiments. Columns, mean; bars, SE.

adhered and suspension 8226/S cells after treatment with the Tipifarnib and Bortezomib combination (Fig 4.6. C). Once again, however, stroma-adhered tumor cells were partially protected. A similar trend was observed in U937 leukemia cells (Fig 4.6 D).

To determine whether HS-5 stromal cells could also protect primary tumor isolates, primary multiple myeloma and AML cells were adhered to HS-5 stroma and treated with the Tipifarnib and Bortezomib combination (Fig 4.7 A and B). Similar to our observations in tumor cell lines, stroma-adhered primary isolates were partially protected relative to suspension cells, whereas fibronectin-adhered tumor cells seemed more sensitive. Stromal cells derived from a multiple myeloma and two AML patients were also able to prevent apoptosis of adhered 8226/S and U937 cells, respectively (Fig 4.7 C-E).

4.3.6 HS-5 bone marrow stromal cells secrete a protective soluble factor.

Partial resistance provided by bone marrow stromal cells could be explained by either CAM-DR or by the participation of protective soluble factors. To address these two possibilities, 8226/S myeloma cells (Fig 4.8 A) and U937 leukemia cells (Fig 4.8 B) were treated with the combination of Tipifarnib and Bortezomib either in suspension culture (suspension), after adhesion to HS-5 stromal cells (coculture), or with separation between the two populations using a transwell insert (transwell). As described previously, stroma-adhered tumor cells were less sensitive to the drug combination when compared with cells treated in suspension (36-hour incubation). Interestingly, tumor cells separated from

stromal cells using a transwell insert remained protected. These results imply that HS-5 cells produce a soluble factor(s) that can attenuate the toxicity of Tipifarnib and Bortezomib. To determine whether tumor-stroma contact enhanced the production of this factor(s), tumor cells were adhered to HS-5 stromal cells and additional tumor cells were separated from coculture by a transwell insert (coculture/transwell). The nonadhered tumor cells were protected similarly to tumor cells separated by the transwell insert (no coculture), suggesting that HS-5 cells constitutively secrete a protective soluble factor(s), and its production is not enhanced by tumor-stroma contact.

4.4 Discussion

The emergence of drug resistance continues to be a major obstacle to the successful treatment of patients with multiple myeloma and AML. Acquired drug resistance is contingent upon the survival of tumor cells during their initial exposure to cancer chemotherapy (*de novo* drug resistance). The interaction between tumor cells and components of their microenvironment remains critical during this early phase of treatment. Environment-mediated resistance is a result of both physical contact between tumor cells and environmental components as well as the exposure of tumor cells to soluble factors. Both of these interactions participate in prosurvival processes that allow tumor cells to resist chemotherapy and acquire multidrug resistance (Hazlehurst et al. 2003, Nefedova et al. 2003).

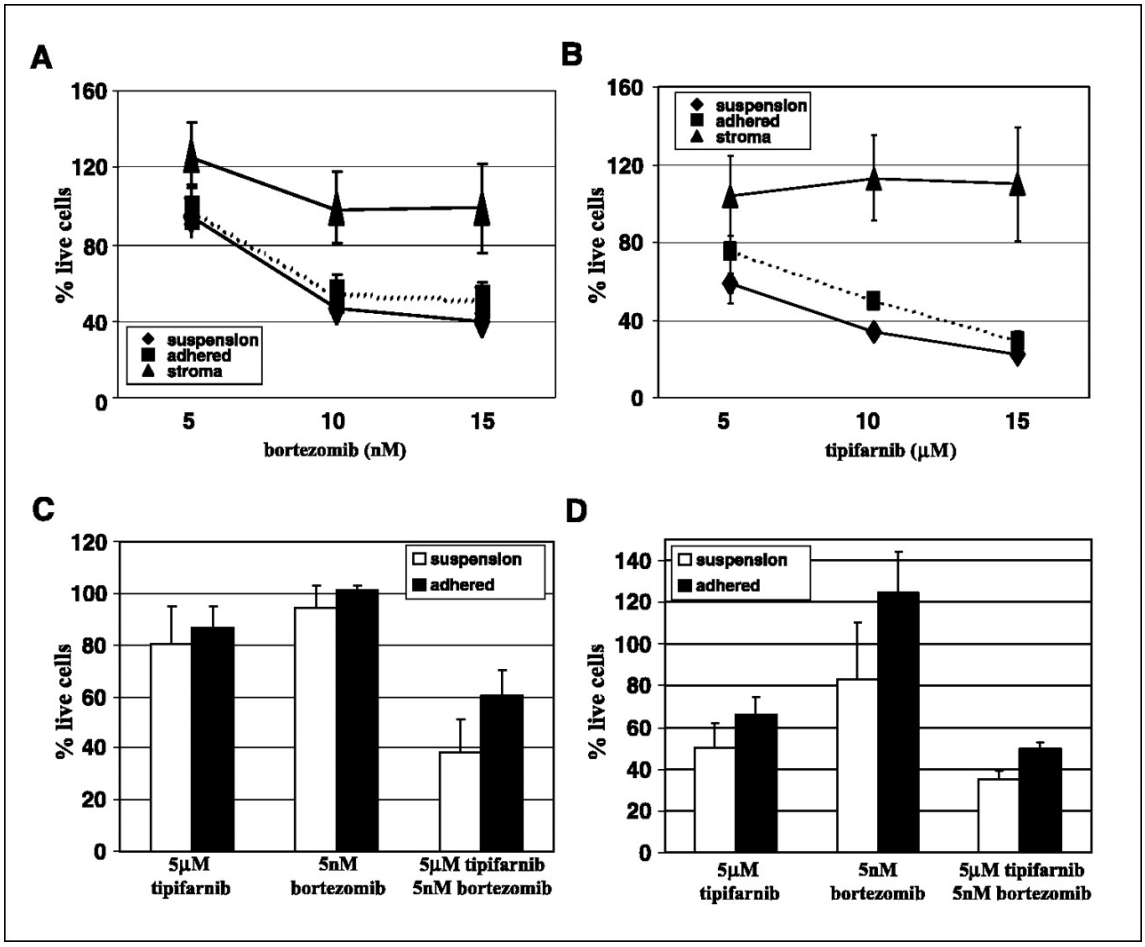

Fig. 4.6 Bone marrow stroma partially protects multiple myeloma and AML cell lines from Tipifarnib- and Bortezomib-induced cell death. 8226/S myeloma cells were treated with the indicated concentrations of Bortezomib (*A*), Tipifarnib (*B*), or the combination (*C*) for 24 hours. Cells were treated either in suspension culture (suspension) or after adhesion to HS-5 stromal cells (adhered). The HS-5 stroma line (stroma) expresses GFP in a stable fashion. Myeloma cells were distinguished from stromal cells in coculture by using flow cytometry with gating on GFP^+ and GFP^- populations. *D*, U937 leukemia cells were treated and analyzed as in (*C*). Cell death was determined by staining with Annexin V/FITC and 7-amino actinomycin-D as described in Materials and Methods. Percent live cells are relative to tumor cells treated with control media only. Combined from three independent experiments (*A-D*). Columns/points, mean; bars, SE.

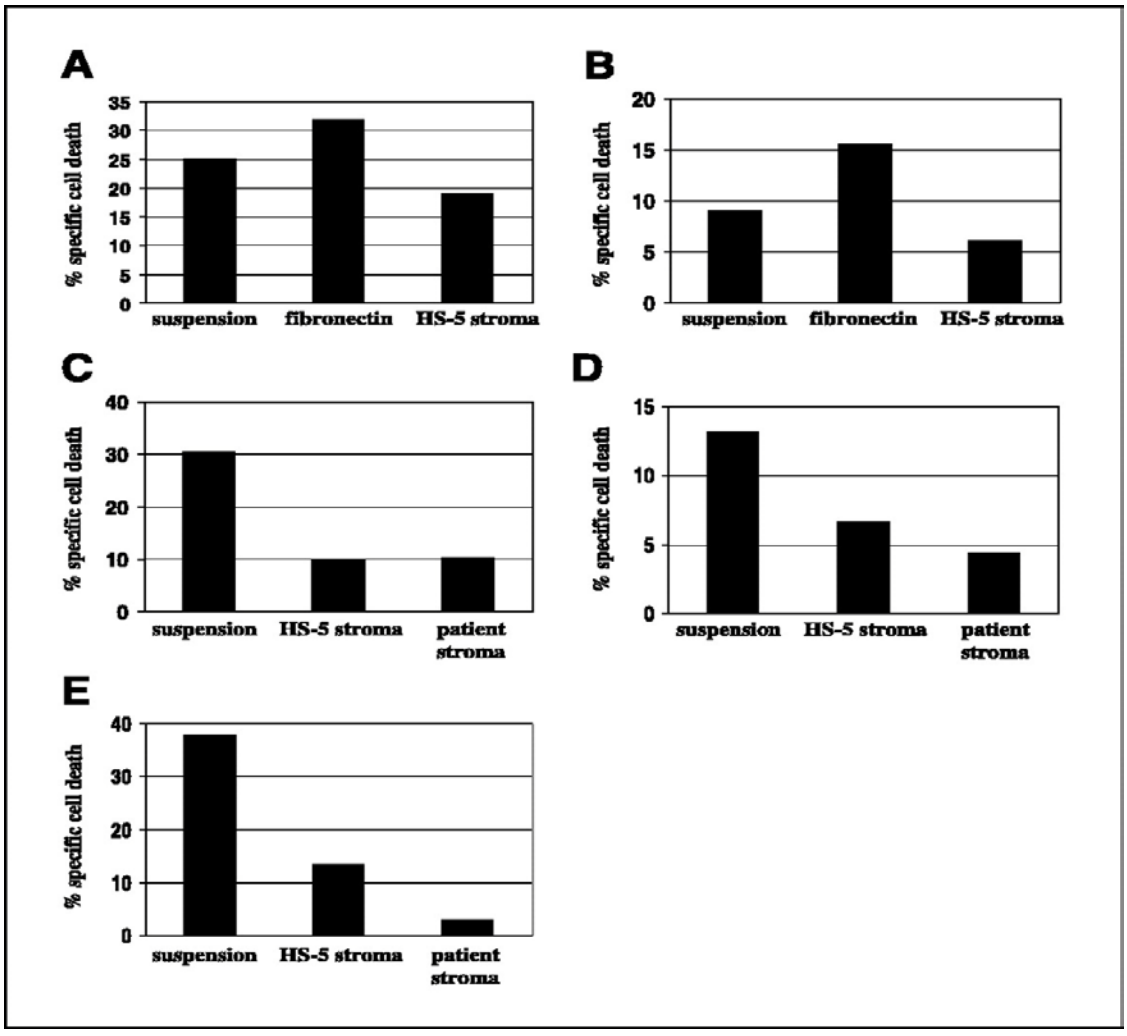

Fig. 4.7 Stromal cells partially protect primary isolates from the Tipifarnib and Bortezomib combination. After obtaining informed consent for bone marrow aspiration, mononuclear cells from a multiple myeloma (*A*) and an AML (*B*) patient were isolated by Ficoll-Hypaque gradient purification. Cells were treated with the combination of 5 μmol/L Tipifarnib and 5 nmol/L Bortezomib for 36 hours either in suspension or after adhesion to fibronectin or HS-5 bone marrow stromal cells. Cell death was determined by flow cytometry after Annexin V/FITC and 7-amino actinomycin-D staining. Tumor cells were identified in coculture by staining with anti-CD138 (myeloma cells) or anti-CD33 (leukemic cells) antibodies. 8226/S myeloma cells (*C*) and U937 leukemic cells (*D* and *E*) were adhered to HS-5 stroma and bone marrow stromal cells derived from a patient with multiple myeloma (*C*) and AML (*D* and *E*), respectively. Tumor cells were exposed to 5 μmol/L Tipifarnib and 5 nmol/L Bortezomib for 36 hours, and cell death was determined as described above. Cell death in adhered samples was compared with tumor cell lines treated in suspension culture. Columns, mean; bars, SE.

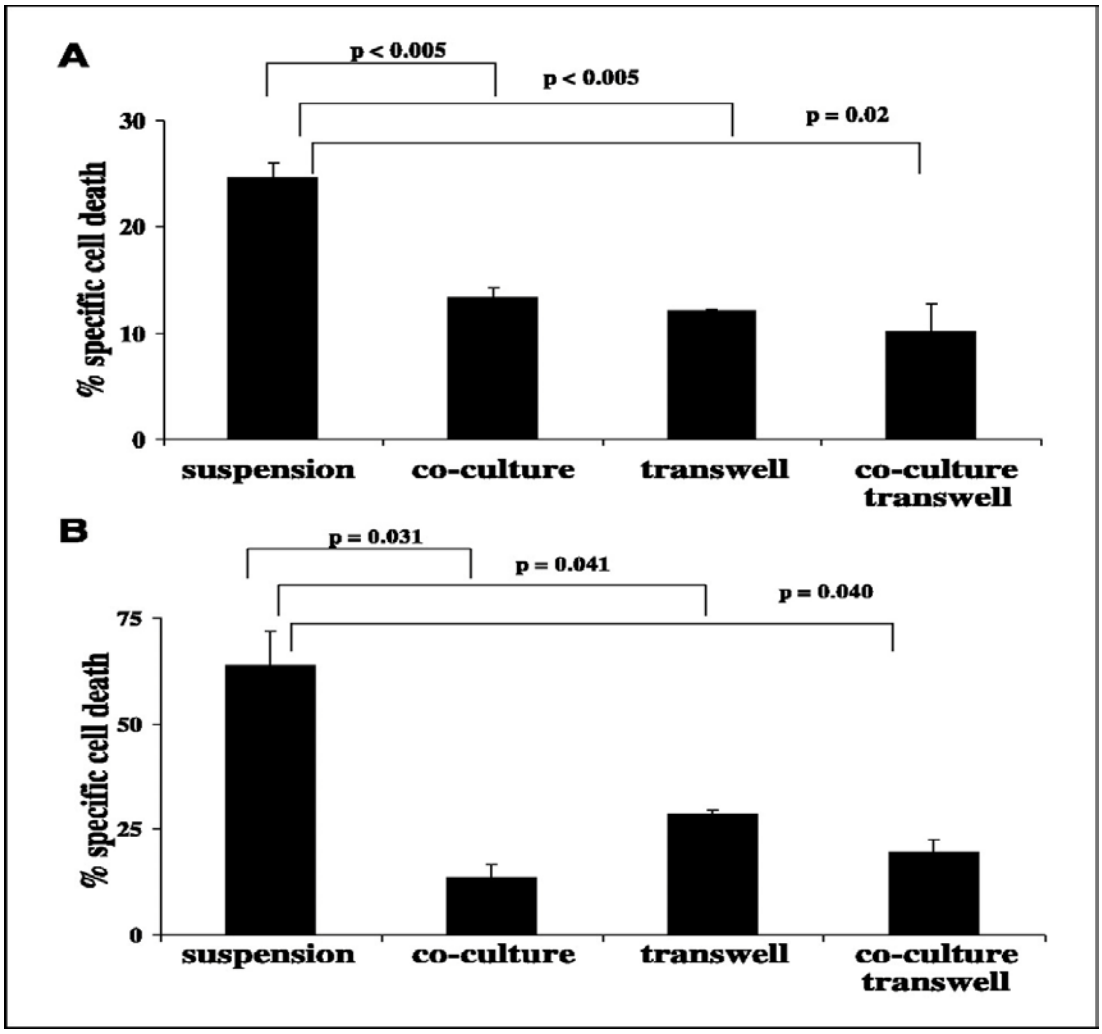

Fig. 4.8 HS-5 stromal cells secrete a soluble factor(s) that protects multiple myeloma and AML cell lines. 8226/S myeloma (*A*) and U937 leukemia cells (*B*) were treated with 5 μmol/L Tipifarnib and 5 nmol/L Bortezomib for 36 hours. Tumor cells were maintained as follows: in suspension culture (suspension), adhered to HS-5 GFP stromal cells (coculture), separated from HS-5 GFP stromal cells by a transwell insert (transwell), or adhered to HS-5 GFP stromal cells with additional tumor cells separated by a transwell insert (coculture/transwell). In the latter sample, nonadhered tumor cells were harvested for evaluation. Cell death was determined by flow cytometry after staining with Annexin V/FITC and 7-amino actinomycin-D. In coculture, death of myeloma and leukemia cells was determined by gating on GFP^- cells. Combined from three independent experiments (*A* and *B*). Individual conditions were compared using a paired *t* test with *P*s. Columns, mean; bars, SE.

Novel agents or drug combinations that overcome *de novo* drug resistance are eagerly sought. Tipifarnib is a FTI that has clinical activity in multiple myeloma and AML (Alsina et al. 2004, Karp et al. 2001). Interestingly, Tipifarnib accumulates in bone marrow (Karp et al. 2001), a desirable property in hematopoietic malignancies that are dependent on the bone marrow microenvironment. We observed that as a single-agent Tipifarnib can overcome the CAM-DR phenotype in multiple myeloma and AML cell lines (Fig 4.3 A and C) and primary isolates (data not shown). It had previously been reported that Bortezomib shares similar activity in fibronectin-adhered (Mitsiades et al. 2006) and stroma-adhered (Hideshima et al. 2001) MM1s myeloma cells, and consistent with this, we found that Bortezomib efficiently induced cell death in stroma-adhered 8226/S myeloma cells (Fig 4.6 A). Because Bortezomib has been shown to sensitize fibronectin-adhered myeloma cells to chemotherapy-mediated apoptosis (Mitsiades et al. 2003), we set out to discern whether low doses of Bortezomib (5 nmol/L) could enhance the activity of Tipifarnib in microenvironment models of multiple myeloma and AML.

Our data reveal that this combination has activity not only in multiple myeloma and AML cells maintained in suspension culture (Fig 4.1) but also in tumor cells adhered to the extracellular matrix component fibronectin (Fig 4.3), indicating that Tipifarnib combined with Bortezomib effectively overcomes CAM-DR. It has been previously reported that Bortezomib decreases the adhesion of myeloma cells to bone marrow stromal cells (Hideshima et al. 2001). Conversely, Tipifarnib did not reduce the adhesion of AML blasts to either primary bone marrow stroma or human umbilical endothelial cells (Liesveld et al. 2003). In our models, Tipifarnib, Bortezomib, nor the combination

decreased tumor cell adhesion to fibronectin implying that cell death was not associated with the loss of tumor-microenvironment contact (Fig 4.4). Stroma-adhered tumor cells were also sensitive to the combination, although they were partially protected relative to cells maintained in suspension culture (Fig 4.6 and 4.7). The fact that Tipifarnib and Bortezomib were particularly active in fibronectin-adhered tumor cells leads us to consider soluble factors as a possible source of stroma-mediated resistance. In experiments where tumor cells were physically separated from stromal cells using a transwell insert, protection persisted confirming that a soluble factor(s) could partially suppress the activity of the drug combination (Fig 4.8).

Several key cytokines serve as autocrine and paracrine growth factors for multiple myeloma and AML cells. IL-6 is known to be a major growth and survival factor in multiple myeloma (Hallek et al. 1998). IL-6 is secreted by HS-5 bone marrow stromal cells (Roecklein et al. 1995) and protects multiple myeloma cells from dexamethasone-mediated apoptosis (Chauhan et al. 2000). Of importance, it has been reported that IL-6 is incapable of protecting myeloma cells from Bortezomib-induced cell death (Hideshima et al. 2001). It therefore remains possible that other cytokines and/or growth factors are involved. HS-5 stromal cells also secrete IL-1ß that can contribute to autocrine and paracrine growth loops in multiple myeloma (Kawano et al. 1989, Nagata et al. 1991) and AML (Sakai et al. 1987, Cozzolino et al. 1989). However, we previously reported that an FTI inhibits the expression of IL-1ß in leukemic cell lines (Beupre et al. 1999), implying that IL-1ß is not the protective cytokine in our models. Vascular endothelial growth factor has also been shown to promote the growth of multiple myeloma (Podar et al. 2001) and

AML cells (List et al. 2004), and its mRNA is expressed in HS-5 stromal cells (Roecklein et al. 1995). It remains to be seen whether any of the abovementioned cytokines are relevant to the observed stromal-mediated resistance, but experiments are under way to define the cytokine(s) and/or growth factor(s) involved. Our findings will have clinical relevance for antagonists to all three of these factors, as well as other soluble proteins are being clinically tested.

With respect to the mechanism of action of this drug combination, as single agents, both Tipifarnib and Bortezomib have been shown to induce ER stress–related apoptosis (Beaupre et al. 2004, Lee et al. 2003, Landowski et al. 2005, Fribley et al. 2004). We found that the combination enhanced activation of the ER stress marker GADD153 (Fig 4.5 C), and this correlated with apoptosis and reversal of CAM-DR. We have previously observed that Tipifarnib increases the expression and activity of Bax (Beaupre et al. 2004) and Bim in myeloma cell lines. Interestingly, it has been reported that the expression of Bax and Bim can be regulated via a proteasome-mediated pathway (Luciano et al. 2003, Li et al. 2000). It therefore remains possible that Tipifarnib and Bortezomib cooperate to enhance the activity of these proapoptotic proteins. Bax and Bim are known to target the ER, leading to ER calcium release (Scorrano et al. 2003), activation of caspase-12 (Morishima et al. 2003, and apoptosis in a mitochondria-independent fashion (Morishima et al. 2002). Mitochondrial dysfunction also occurs after Tipifarnib treatment (Beaupre et al. 2004) and is likely the result of localization of Bax and Bim to mitochondria. It remains possible, however, that intracytoplasmic calcium participates in mitochondrial membrane depolarization by opening of the mitochondrial

permeability transition pore (Landowshi et al. 2005, Rizzuot et al. 2003). Importantly, Tipifarnib and Bortezomib are active when tumor cells are adhered to fibronectin. Bim expression is known to decrease in adhered myeloma cells (Hazlehurst et al. 2003), and it remains possible that the combination reverses this effect. Current investigations are determining the role of Bax and Bim in reversal of the CAM-DR phenotype. Delineation of the ER stress–related mechanisms responsible for Tipifarnib and Bortezomib combined activity may ultimately lead to treatment strategies that specifically target environment-mediated drug resistance.

In conclusion, in this study, we provide the preclinical rationale for clinical trials testing Tipifarnib and Bortezomib in patients with multiple myeloma and AML. Future trials may also include a cytokine and/or growth factor neutralization strategy once protective soluble factors are identified. In theory, such a regimen would eradicate tumor cells protected by the microenvironment compartment, leaving sensitive tumor cell populations for standard or high-dose chemotherapy.

Chapter 5

Summary and Major Conclusions

5.1 Identification and characterization of the R115777 resistant cell line

The farnesyl transferase inhibitor R115777 has been found to have clinical activity in diverse hematopoietic tumors. Clinical efficacy, however, does not correlate with Ras mutation status or inhibition of farnesyl transferase. To further elucidate the mechanisms by which R115777 induces apoptosis and to investigate drug resistance, we identified and characterized a R115777-resistant human myeloma cell line. 8226/R5 cells were found to be at least 50 times more resistant to R115777 compared with the parent cell line 8226/S. K-Ras remained prenylated in both resistant and sensitive cells after R115777 treatment; however, HDJ-2 farnesylation was inhibited in both lines, implying that farnesyl transfeRase (the drug target) has not been mutated. Whereas many 8226 lines that acquire drug resistance have elevated expression of P-glycoprotein, we found that P-glycoprotein expression is not increased in the 8226/R5 line and intracellular accumulation of R115777 was not reduced. In fact, 8226/R5 cells were insensitive to a diverse group of antitumor agents including PS-341, and multidrug resistance did not correlate with the expression of heat shock proteins. Comparison of gene expression

profiles between resistant and sensitive cells revealed expression changes in several genes involved in myeloma survival and drug resistance. Identification of molecules associated with R115777 and PS-341 resistance is clinically relevant because both compounds are being tested in solid tumors and hematopoietic malignancies.

5.2 The role of the Akt survival pathway in R115777 induced apoptosis and resistance

It has been well described that R115777 induces apoptosis in a RAS-independent manner. In this study I have implicated Akt as a possible culprit in the cytotxic resistance to R115777. I have demonstrated that Tipifarnib induces apoptosis in myeloma cell lines when AKT in not endogenously active. As such, we were able to correlate levels of pAkt expression to drug resistance in multiple myeloma in cell lines. In MM primary isolates, AKT has been found to be predominately activated and localized to the nucleus. However, no direct correlation between Akt localization and drug resistance has yet been characterized until now. Here we have demonstrated a correlation between nuclear localization of pAkt and drug resistance in MM cells. Utalizing a SCID-hu model of myeloma we were successful in exhibiting the *in vivo* cytoxicity of myeloma cells from R115777.

5.3 Combination treatment using R15777 and PS-341

It has been established in preclinical models of multiple myeloma and acute myeloid leukemia (AML) that the bone marrow microenvironment provides protection

from chemotherapy- and death receptor–mediated apoptosis. This form of resistance, termed de novo drug resistance, occurs independent of chronic exposure to cancer-related therapies and likely promotes the development of multidrug resistance. Consequently, it is of major interest to identify compounds or drug combinations that can overcome environment-mediated resistance. In this study, we investigated the activity of Tipifarnib (Zarnestra, formerly R115777) combined with Bortezomib (Velcade, formerly PS-341) in microenvironment models of multiple myeloma and AML. The combination proved to be synergistic in multiple myeloma and AML cell lines treated in suspension culture. Even in tumor cells relatively resistant to Tipifarnib, combined activity was maintained. Tipifarnib and Bortezomib were also effective when multiple myeloma and AML cells were adhered to fibronectin, providing evidence that the combination overcomes cell adhesion–mediated drug resistance (CAM-DR). Of importance, activation of the endoplasmic reticulum stress response was enhanced and correlated with apoptosis and reversal of CAM-DR. Multiple myeloma and AML cells cocultured with bone marrow stromal cells also remained sensitive, although stromal-adhered tumor cells were partially protected (relative to cells in suspension or fibronectin adhered). Evaluation of the combination using a transwell apparatus revealed that stromal cells produce a protective soluble factor. Investigations are under way to identify the cytokines and/or growth factors involved. In summary, our study provides the preclinical rationale for trials testing the Tipifarnib and Bortezomib combination in patients with multiple myeloma and AML.

Literature Cited

Adini I, Rabinovitz I, Sun JF, Prendergast GC, Benjamin LE. RhoB controls Akt trafficking and stage-specific survival of endothelial cells during vascular development. Genes & development. 2003 Nov 1;17(21):2721-32.

Alas S, Bonavida B. Inhibition of constitutive STAT3 activity sensitizes resistant non-Hodgkin's lymphoma and multiple myeloma to chemotherapeutic drug-mediated apoptosis. Clin Cancer Res 2003;9:316–26.

Alkan S, Izban KF. Immunohistochemical localization of phosphorylated AKT in multiple myeloma. Blood. 2002 Mar 15;99(6):2278-9.

Alsina M, Fonseca R, Wilson EF, et al. The farnesyltransferase inhibitor Zarnestra is well tolerated, induces stabilization of disease and inhibits farnesylation and oncogenic/tumor survival pathways in patients with advanced multiple myeloma. Blood 2004;103:3271–7.

Badros A, Goloubeva O, Dalal JS, Can I, Thompson J, Rapoport AP, Heyman M, Akpek G, Fenton RG. Neurotoxicity of Bortezomib therapy in multiple myeloma: a single-center experience and review of the literature. Cancer. Sep 1;110(5):1042-9 (2007)

Bauduer F, Troussard X, Delmer A. Prognostic factors in multiple myeloma. Review of the literature. Bull Cancer 1993;80:1035–42.

Beaupre DM, Cepero E, Obeng EA, Boise LH, Lichtenheld MG. R115777 induces Ras-independent apoptosis of myeloma cells via multiple intrinsic pathways. Mol Cancer Ther 2004;3:179–86.

Beaupre DM, McCafferty-Grad J, Bahlis NJ, Boise LH, Lichtenheld MG. Farnesyl transferase inhibitors enhance death receptor signals and induce apoptosis in multiple myeloma cells. Leuk Lymphoma 2003;44:2123–34.

Beaupre DM, Talpaz M, Marini FC, III, et al. Autocrine interleukin-1ß production in leukemia: evidence for the involvement of mutated RAS. Cancer Res 1999;59:2971–80.

Bergsagel D. The incidence and epidemiology of plasma cell neoplasms. Stem cells (Dayton, Ohio). 1995 Aug;13 Suppl 2:1-9.

Bezieau S, Devilder MC, Avet-Loiseau H, et al. High incidence of N- and K-Ras activating mutations in multiple myeloma and primary plasma cell leukemia at diagnosis. Hum Mutat 2001;18:212–24.

Bharti AC, Shishodia S, Reuben JM, et al. Nuclear factor-κB and STAT3 are constitutively active in $CD138^+$ cells derived from multiple myeloma patients, and suppression of these transcription factors leads to apoptosis. Blood 2004;103:3175–84.

Bolick SC, Landowski TH, Boulware D, et al. The farnesyl transferase inhibitor, FTI-277, inhibits growth and induces apoptosis in drug-resistant myeloma tumor cells. Leukemia 2003;17:451–7.

Brunet A, Bonni A, Zigmond MJ, Lin MZ, Juo P, Hu LS, et al. Akt promotes cell survival by phosphorylating and inhibiting a Forkhead transcription factor. Cell. 1999 Mar 19;96(6):857-68.

Brunner TB, Hahn SM, Gupta AK, Muschel RJ, Mckenna WG, Bernhard EJ. FarnesyltransfeRase inhibitors: An overview of the results of preclinical and clinical investigations. Cancer Research. 2003. 64, 565605668

Buzzeo R, Enkemann S, Nimmanapalli R, Alsina M, Lichtenheld MG, Dalton WS, et al. Characterization of a R115777-resistant human multiple myeloma cell line with cross-resistance to PS-341. Clin Cancer Res. 2005 Aug 15;11(16):6057-64.

Cantley LC. The phosphoinositide 3-kinase pathway. Science. 2002 May 31;296(5573):1655-7.

Catlett-Falcone R, Landowski TH, Oshiro MM, et al. Constitutive activation of Stat3 signaling confers resistance to apoptosis in human U266 myeloma cells. Immunity 1999;10:105–15.

Chantry D, Vojtek A, Kashishian A, et al. p110δ, a novel phosphatidylinositol 3-kinase catalytic subunit that associates with p85 and is expressed predominantly in leukocytes. J Biol Chem 1997;272:19236–41.

Chauhan D, Li G, Auclair D, et al. 2-Methoxyestardiol and bortezomib/proteasome-inhibitor overcome dexamethasone-resistance in multiple myeloma cells by modulating Heat Shock Protein-27. Apoptosis 2004;9:149–55.

Chauhan D, Li G, Shringarpure R, et al. Blockade of Hsp27 overcomes Bortezomib/proteasome inhibitor PS-341 resistance in lymphoma cells. Cancer Res 2003;63:6174–7.

Chauhan D, Pandey P, Hideshima T, et al. SHP2 mediates the protective effect of interleukin-6 against dexamethasone-induced apoptosis in multiple myeloma cells. J Biol Chem 2000;275:27845–50.

Chou TC, Talalay P. Quantitative analysis of dose-effect relationships: the combined effects of multiple drugs or enzyme inhibitors. Adv Enzyme Regul 1984;22:27–55.

Corradini P, Ladetto M, Inghirami G, et al. N- and K-*ras* oncogenes in plasma cell dyscrasias. Leuk Lymphoma 1994;15:17–20.

Cortes J, Albitar M, Thomas D, et al. Efficacy of the farnesyl transferase inhibitor R115777 in chronic myeloid leukemia and other hematologic malignancies. Blood 2003;101:1692–7.

Cortes JE, Kurzrock R, Kantarjian HM. Farnesyltransferase inhibitors: novel compounds in development for the treatment of myeloid malignancies. Seminars in hematology. 2002 Jul;39(3 Suppl 2):26-30.

Cox AD. Farnesyltransferase inhibitors: potential role in the treatment of cancer. Drugs. 2001;61(6):723-32.

Cozzolino F, Rubartelli A, Aldinucci D, et al. Interleukin 1 as an autocrine growth factor for acute myeloid leukemia cells. Proc Natl Acad Sci U S A 1989;86:2369–73.

Cunningham D, de Gramount A, Scheithauer W, Smakal M, Humblet Y, Kurteva G, Ivenson T, Andre T, Dostalova J, Illes A, Jia X, Palmer P. Randomized double-blind placebo controlled trial of the farnesyltransfeRase inhibitor R115777 (Zarnestra) in advanced refractory colorectal cancer (PC). Proc. Am. Soc. Clin. Oncol. 21:502, 2002

Dai Y, Rahmani M, Grant S. Proteasome inhibitors potentiate leukemic cell apoptosis induced by the cyclin-dependent kinase inhibitor flavopiridol through a SAPK/JNK- and NF-κB-dependent process. Oncogene 2003;22:7108–22.

Daley GQ, Baltimore D. Transformation of an interleukin 3-dependent hematopoietic cell line by the chronic myelogenous leukemia-specific P210bcr/abl protein. Proceedings of the National Academy of Sciences of the United States of America. 1988 Dec;85(23):9312-6.

Dalton WS, Durie BG, Alberts DS, et al. Characterization of a new drug-resistant human myeloma cell line that expresses P-glycoprotein. Cancer Res 1986;46:5125–30.

Dalton WS. Mechanisms of drug resistance in hematologic malignancies. Seminars in hematology. 1997 Oct;34(4 Suppl 5):3-8.

Damiano JS, Cress AE, Hazlehurst LA, Shtil AA, Dalton WS. Cell adhesion mediated drug resistance (CAM-DR): role of integrins and resistance to apoptosis in human myeloma cell lines. Blood 1999;93:1658–67.

Dominik D. Alexander, Pamela J. Mink, Hans-Olov Adami, Phillip Cole, Jack Mandel, Martin M. Oken and Dimitrios Trichopoulos. Multiple myeloma: A review of the epidemiologic literature. Int. J. Cancer: 120, 40-61 (2007)

Du W, Liu A, Prendergast GC. Activation of the PI3'K-AKT pathway masks the proapoptotic effects of farnesyltransferase inhibitors. Cancer Res. 1999 Sep 1;59(17):4208-12.

DuHadaway JB, Du W, Donover S, Baker J, Liu AX, Sharp DM, et al. Transformation-selective apoptotic program triggered by farnesyltransferase inhibitors requires Bin1. Oncogene. 2003 Jun 5;22(23):3578-88.

End DW, Smets G, Todd AV, et al. Characterization of the antitumor effects of the selective farnesyl protein transferase inhibitor R115777 *in vivo* and *in vitro*. Cancer Res 2001;61:131–7.

Franke TF, Yang SI, Chan TO, Datta K, Kazlauskas A, Morrison DK, et al. The protein kinase encoded by the Akt proto-oncogene is a target of the PDGF-activated phosphatidylinositol 3-kinase. Cell. 1995 Jun 2;81(5):727-36.

Fribley A, Zeng Q, Wang CY. Proteasome inhibitor PS-341 induces apoptosis through induction of endoplasmic reticulum stress-reactive oxygen species in head and neck squamous cell carcinoma cells. Mol Cell Biol 2004;24:9695–704.

Gelb MH, Tamanoi F, Yokoyama K, et al. The inhibition of protein prenyltransferases by oxygenated metabolites of limonene and perillyl alcohol. Cancer Lett 1995;91:169–75.

Ghafoor A, Jemal A, Cokkinides V, Cardinez C, Murray T, Samuels A, et al. Cancer statistics for African Americans. CA: a cancer journal for clinicians. 2002 Nov-Dec;52(6):326-41.

Grad JM, Zeng XR, Boise LH. Regulation of Bcl-xL: a little bit of this and a little bit of STAT. Curr Opin Oncol 2000;12:543–9.

Hahn SM, Bernhard E, McKenna WG. Farnesyltransferase inhibitors. Seminars in oncology. 2001 Oct;28(5 Suppl 16):86-93.

Hallek M, Bergsagel PL, Anderson KC. Multiple myeloma: increasing evidence for a multistep transformation process. Blood. 1998 Jan 1;91(1):3-21.

Hancock JF, Magee AI, Childs JE, Marshall CJ. All ras proteins are polyisoprenylated but only some are palmitoylated. Cell. 1989 Jun 30;57(7):1167-77.

Hanks SK, Calab MB, Harper MC, Patel SK: Focal adhesion protein-tyrosine kinase phosphorylated in response to cell spreading on fibronectin. Proc Natl Acad Sci 89: 8487-8491, 1992

Hazlehurst LA, Enkemann SA, Beam CA, et al. Genotypic and phenotypic comparisons of *de novo* and acquired melphalan resistance in an isogenic multiple myeloma cell line model. Cancer Res 2003;63:7900–6.

Hazlehurst LA, Landowski TH, Dalton WS. Role of the tumor microenvironment in mediating *de novo* resistance to drugs and physiological mediators of cell death. Oncogene 2003;22:7396–402.

Hideshima T, Nakamura N, Chauhan D, et al. Biologic sequelae of interleukin-6 induced PI3-K/Akt signaling in multiple myeloma. Oncogene 2001;20:5991–6000.

Hideshima T, Richardson P, Chauhan D, et al. The proteasome inhibitor PS-341 inhibits growth, induces apoptosis, and overcomes drug resistance in human multiple myeloma cells. Cancer Res 2001;61:3071–6.

Hiles ID, Otsu M, Volinia S, et al. Phosphatidylinositol 3-kinase: structure and expression of the 110 kd catalytic subunit. Cell 1992;70:419–29.

Hsu JH, Shi Y, Hu L, et al. Role of the AKT kinase in expansion of multiple myeloma clones: effects on cytokine-dependent proliferative and survival responses. Oncogene 2002;21:1391–400.

Hu W, Wu W, Verschraegen CF, et al. Proteomic identification of heat shock protein 70 as a candidate target for enhancing apoptosis induced by farnesyl transferase inhibitor. Proteomics 2003;3:1904–11.

Huang HM, Lin YL, Chen CH, Chang TW. Simultaneous activation of JAK1 and JAK2 confers IL-3 independent growth on Ba/F3 pro-B cells. Journal of cellular biochemistry. 2005 Oct 1;96(2):361-75.

Jiang K, Coppola D, Crespo NC, et al. The phosphoinositide 3-OH kinase/AKT2 pathway as a critical target for farnesyltransferase inhibitor-induced apoptosis. Mol Cell Biol 2000;20:139–48.

Kane RC, Bross PF, Farrell AT, Pazdur R. Velcade: U.S. FDA approval for the treatment of multiple myeloma progressing on prior therapy. Oncologist 2003;8:508–13.

Karp JE, Lancet JE, Kaufmann SH, et al. Clinical and biologic activity of the farnesyltransferase inhibitor R115777 in adults with refractory and relapsed acute leukemias: a phase 1 clinical-laboratory correlative trial. Blood 2001;97:3361–9.

Kato K, Cox AD, Hisaka MM, Graham SM, Buss JE, Der CJ. Isoprenoid addition to Ras protein is the critical modification for its membrane association and transforming activity. Proceedings of the National Academy of Sciences of the United States of America. 1992 Jul 15;89(14):6403-7.

Kawano M, Tanaka H, Ishikawa H, et al. Interleukin-1 accelerates autocrine growth of myeloma cells through interleukin-6 in human myeloma. Blood 1989;73:2145–8.

Keating A. Chronic myeloid leukemia: current therapies and the potential role of farnesyltransferase inhibitors. Semin Hematol 2002;39:11–7.

Kelland LR, Smith V, Valenti M, Patterson L, Clarke PA, Detre S, et al. Preclinical antitumor activity and pharmacodynamic studies with the farnesyl protein transferase inhibitor R115777 in human breast cancer. Clin Cancer Res. 2001 Nov;7(11):3544-50.

King WG, Maytaliano CTO, Tsichilis PN, Brugge JS, Phosphatidylinosital 3-kinase is required for integrin-stimulated AKT and RAF-1/mitogen-activated protein kinase pathway activation. Mol Cell Biol 17:4406-4418, 1997

Kurzrock R, Cortes J, Kantarjian H. Clinical development of farnesyltransferase inhibitors in leukemias and myelodysplastic syndrome. Semin Hematol 2002;39:20–4.

Kyle R. Rajkumar V. Multiple Myeloma. The New England Journal of Medicine. Volume 351:1860-1873 (2004)

Landowski TH, Megli CJ, Nullmeyer KD, Lynch RM, Dorr RT. Mitochondrial-mediated disregulation of C^{a2+} is a critical determinant of Velcade (PS-341/bortezomib) cytotoxicity in myeloma cell lines. Cancer Res 2005;65:3828–36.

Lavie Y, Liscovitch M. Changes in lipid and protein constituents of rafts and caveolae in multidrug resistant cancer cells and their functional consequences. Glycoconj J 2000;17:253–9.

Le Gouill S, Pellat-Deceunynck C, Harousseau JL, et al. Farnesyl transferase inhibitor R115777 induces apoptosis of human myeloma cells. Leukemia 2002;16:1664–7.

Lebowitz PF, Eng-Wong J, Widemann BC, Balis FM, Jayaprakash N, Chow C, et al. A phase I trial and pharmacokinetic study of tipifarnib, a farnesyltransferase inhibitor, and tamoxifen in metastatic breast cancer. Clin Cancer Res. 2005 Feb 1;11(3):1247-52.

LeCouter J, Zlot C, Tejada M, Peale F, Ferrara N. Bv8 and endocrine gland-derived vascular endothelial growth factor stimulate hematopoiesis and hematopoietic cell mobilization. Proc Natl Acad Sci U S A 2004;101:16813–8.

Lee AH, Iwakoshi NN, Anderson KC, Glimcher LH. Proteasome inhibitors disrupt the unfolded protein response in myeloma cells. Proc Natl Acad Sci U S A 2003;100:9946–51.

Lee JW, Juliano RL: Alpha 5 beta 1 integrin protects intestinal epithelial cells from apoptosis through a phosphatidylinositol 3-kinase and protein kinase B-dependent pathway. Mol Biol Cell 11: 1973-1987, 2000

Lerner EC, Qian Y, Blaskovich MA, et al. Ras CAAX peptidomimetic FTI-277 selectively blocks oncogenic Ras signaling by inducing cytoplasmic accumulation of inactive Ras-Raf complexes. J Biol Chem 1995;270:26802–6.

Li B, Dou QP. Bax degradation by the ubiquitin/proteasome-dependent pathway: involvement in tumor survival and progression. Proc Natl Acad Sci U S A 2000;97:3850–5.

Liesveld JL, Lancet JE, Rosell KE, et al. Effects of the farnesyl transferase inhibitor R115777 on normal and leukemic hematopoiesis. Leukemia 2003;17:1806–12.

Lin TH, Aplin AE, Shen Y, Chen Q, Schaller M, Romer L, Aukhil I, Juliano RL: Integrin-mediated activation of MAP kinase is independent of FAK: Evidence for dual integrin signaling pathways in fibroblasts. J Cell Biol 136: 1385-1395, 1997

List AF, Glinsmann-Gibson B, Stadheim C, Meuillet EJ, Bellamy W, Powis G. Vascular endothelial growth factor receptor-1 and receptor-2 initiate a phosphatidylinositide 3-kinase-dependent clonogenic response in acute myeloid leukemia cells. Exp Hematol 2004;32:526–35.

Liu P, Leong T, Quam L, Billadeau D, Kay NE, Greipp P, et al. Activating mutations of N- and K-ras in multiple myeloma show different clinical associations: analysis of the Eastern Cooperative Oncology Group Phase III Trial. Blood. 1996 Oct 1;88(7):2699-706.

Liu WM, Mei R, Di X, et al. Analysis of high density expression microarrays with signed-rank call algorithms. Bioinformatics 2002;18:1593–9.

Luciano F, Jacquel A, Colosetti P, et al. Phosphorylation of Bim-EL by Erk1/2 on serine 69 promotes its degradation via the proteasome pathway and regulates its proapoptotic function. Oncogene 2003;22:6785–93.

Ma MH, Yang HH, Parker K, et al. The proteasome inhibitor PS-341 markedly enhances sensitivity of multiple myeloma tumor cells to chemotherapeutic agents. Clin Cancer Res 2003;9:1136–44.

Madrid LV, Wang CY, Guttridge DC, Schottelius AJ, Baldwin AS, Jr., Mayo MW. Akt suppresses apoptosis by stimulating the transactivation potential of the RelA/p65 subunit of NF-kappaB. Molecular and cellular biology. 2000 Mar;20(5):1626-38.

Matsunaga T, Takemoto N, Sato T, et al. Interaction between leukemic-cell VLA-4 and stromal fibronectin is a decisive factor for minimal residual disease of acute myelogenous leukemia. Nat Med 2003;9:1158–65.

Meng F, Lowell CA: A beta 1 integrin signaling pathway involving Src-family kinases, Cbl and Pi-3 kinase is required for macrophage spreading and migration. EMBO J 17: 4391-4403, 1998

Mitsiades N, Mitsiades CS, Richardson PG, et al. The proteasome inhibitor PS-341 potentiates sensitivity of multiple myeloma cells to conventional chemotherapeutic agents: therapeutic applications. Blood 2003;101:2377–80.

Morishima N, Nakanishi K, Takenouchi H, Shibata T, Yasuhiko Y. An endoplasmic reticulum stress-specific caspase cascade in apoptosis. Cytochrome *c*-independent activation of caspase-9 by caspase-12. J Biol Chem 2002;277:34287–94.

Morishima N, Nakanishi K, Tsuchiya K, Shibata T, Seiwa E. Translocation of Bim to the endoplasmic reticulum (ER) mediates ER stress signaling for activation of caspase-12 during ER stress-induced apoptosis. J Biol Chem 2004;279:50375–81.

Nagata K, Tanaka Y, Oda S, Yamashita U, Eto S. Interleukin 1 autocrine growth system in human multiple myeloma. Jpn J Clin Oncol 1991;21:22–9.

Nefedova Y, Landowski TH, Dalton WS. Bone marrow stromal-derived soluble factors and direct cell contact contribute to *de novo* drug resistance of myeloma cells by distinct mechanisms. Leukemia 2003;17:1175–82.

Neri A, Murphy JP, Cro L, Ferrero D, Tarella C, Baldini L, et al. Ras oncogene mutation in multiple myeloma. The Journal of experimental medicine. 1989 Nov 1;170(5):1715-25.

Ochiai N, Uchida R, Fuchida S, Okano A, Okamoto M, Ashihara E, et al. Effect of farnesyl transferase inhibitor R115777 on the growth of fresh and cloned myeloma cells in vitro. Blood. 2003 Nov 1;102(9):3349-53.

Onishi M, Nosaka T, Misawa K, Mui AL, Gorman D, McMahon M, et al. Identification and characterization of a constitutively active STAT5 mutant that promotes cell proliferation. Molecular and cellular biology. 1998 Jul;18(7):3871-9.

Otsu M, Hiles I, Gout I, et al. Characterization of two 85 kd proteins that associate with receptor tyrosine kinases, middle-T/pp60c-src complexes, and PI3-kinase. Cell 1991;65:91–104.

Palumbo, Gay, Bringhen, Falcone, Pescosta, Callea, Caravita, Morabito, Magarotto, Ruggeri, Avonto, Musto, Cascavilla, Bruno and Boccadoro. Bortezomib, doxorubicin and dexamethasone in advanced multiple myeloma. Annals of Oncology. 19(6):1160-1165. (2008)

Pei XY, Dai Y, Grant S. Synergistic induction of oxidative injury and apoptosis in human multiple myeloma cells by the proteasome inhibitor bortezomib and histone deacetylase inhibitors. Clin Cancer Res. 2004 Jun 1;10(11):3839-52.

Podar K, Tai YT, Davies FE, et al. Vascular endothelial growth factor triggers signaling cascades mediating multiple myeloma cell growth and migration. Blood 2001;98:428–35.

Read MA, Neish AS, Luscinskas FW, Palombella VJ, Maniatis T, Collins T. The proteasome pathway is required for cytokine-induced endothelial-leukocyte adhesion molecule expression. Immunity 1995;2:493–506.

Richardson P, Anderson K. Immunomodulatory analogs of thalidomide: an emerging new therapy in myeloma. J Clin Oncol. 2004 Aug 15;22(16):3212-4.

Rizzuto R, Pinton P, Ferrari D, et al. Calcium and apoptosis: facts and hypotheses. Oncogene 2003;22:8619–27.

Roecklein BA, Torok-Storb B. Functionally distinct human marrow stromal cell lines immortalized by transduction with the human papilloma virus E6/E7 genes. Blood 1995;85:997–1005.

Sakai K, Hattori T, Matsuoka M, et al. Autocrine stimulation of interleukin 1 ß in acute myelogenous leukemia cells. J Exp Med 1987;166:1597–602.

Santucci R, Mackley PA, Sebti S, Alsina M. Farnesyltransferase inhibitors and their role in the treatment of multiple myeloma. Cancer Control. 2003 Sep-Oct;10(5):384-7.

Scorrano L, Oakes SA, Opferman JT, et al. BAX and BAK regulation of endoplasmic reticulum Ca^{2+}: a control point for apoptosis. Science 2003;300:135–9.

Sebti S, Hamilton AD. Inhibitors of prenyl transferases. Current opinion in oncology. 1997 Nov;9(6):557-61.

Sebti SM, Hamilton AD. Farnesyltransferase and geranylgeranyltransferase I inhibitors and cancer therapy: lessons from mechanism and bench-to-bedside translational studies. Oncogene 2000;19:6584–93.

Shain KH, Dalton WS. Cell adhesion is a key determinant in *de novo* multidrug resistance (MDR): new targets for the prevention of acquired MDR. Mol Cancer Ther 2001;1:69–78.

Smith V, Rowlands MG, Barrie E, et al. Establishment and characterization of acquired resistance to the farnesyl protein transferase inhibitor R115777 in a human colon cancer cell line. Clin Cancer Res 2002;8:2002–9.

Sun J, Qian Y, Hamilton AD, Sebti SM. Both farnesyltransferase and geranylgeranyltransferase I inhibitors are required for inhibition of oncogenic K-Ras prenylation but each alone is sufficient to suppress human tumor growth in nude mouse xenografts. Oncogene. 1998 Mar;16(11):1467-73.

Takada Y, Khuri FR, Aggarwal BB. Protein farnesyltransferase inhibitor (SCH 66336) abolishes NF-kappaB activation induced by various carcinogens and inflammatory stimuli leading to suppression of NF-kappaB-regulated gene expression and up-regulation of apoptosis. The Journal of biological chemistry. 2004 Jun 18;279(25):26287-99.

Tamanoi F, Gau CL, Jiang C, Edamatsu H, Kato-Stankiewicz J. Protein farnesylation in mammalian cells: effects of farnesyltransferase inhibitors on cancer cells. Cell Mol Life Sci. 2001 Oct;58(11):1636-49.

Tu Y, Gardner A, Lichtenstein A. The phosphatidylinositol 3-kinase/AKT kinase pathway in multiple myeloma plasma cells: roles in cytokine-dependent survival and proliferative responses. Cancer research. 2000 Dec 1;60(23):6763-70.

Tu Y, Renner S, Xu F, et al. BCL-X expression in multiple myeloma: possible indicator of chemoresistance. Cancer Res 1998;58:256–62.

Urashima M, Chen BP, Chen S, Pinkus GS, Bronson RT, Dedera DA, et al. The development of a model for the homing of multiple myeloma cells to human bone marrow. Blood. 1997 Jul 15;90(2):754-65.

Van Cutsem E, KaRasek P, Oettle H, Vervenne W, Szawlowski A, Schoffskiu P, Post S, Neumann H, Safran H, Humblet Y, van de Velde H, Ma Y, Von Hoff D. Phase III trial comparing gemcitabine + R115777 (Zarnestra versus gemcitabine + Placebo in advanced pancreatic cancer (PC). Proc. Am. Soc. Clin. Oncol. 2002. 21:517

Van der Velde-Zimmermann D, Verdaasdonk MAM, Joling P. Fibronectin distribution in human bone marrow stroma: Matrix assembly and tumor cell adhesion via alpha-5 beta-1 integrin. Exp Cell Research. 1996 Oct 3400-3405

Van Gelder RN, von Zastrow ME, Yool A, et al. Amplified RNA synthesized from limited quantities of heterogeneous cDNA. Proc Natl Acad Sci U S A 1990;87:1663–7.

Vanhaesebroeck B, Welham MJ, Kotani K, et al. P110δ, a novel phosphoinositide 3-kinase in leukocytes. Proc Natl Acad Sci U S A 1997;94:4330–5.

Wang XZ, Lawson B, Brewer JW, et al. Signals from the stressed endoplasmic reticulum induce C/EBP-homologous protein (CHOP/GADD153). Mol Cell Biol 1996;16:4273–80.

Warrington JA, Nair A, Mahadevappa M, et al. Comparison of human adult and fetal expression and identification of 535 housekeeping/maintenance genes. Physiol Genomics 2000;2:143–7.

Weber D. Thalidomide and its derivatives: new promise for multiple myeloma. Cancer Control. 2003 Sep-Oct;10(5):375-83.

Weber DM. Newly diagnosed multiple myeloma. Current treatment options in oncology. 2002 Jun;3(3):235-45.

Willumsen BM, Christensen A, Hubbert NL, Papageorge AG, Lowy DR. The p21 ras C-terminus is required for transformation and membrane association. Nature. 1984 Aug 16-22;310(5978):583-6.

Yanamandra N, Colaco NM, Parquet NA, Buzzeo RW, Boulware D, Wright G, et al. Tipifarnib and bortezomib are synergistic and overcome cell adhesion-mediated drug resistance in multiple myeloma and acute myeloid leukemia.

Zhu K, Gerbino E, Beaupre DM, Mackley PA, Muro-Cacho C, Beam C, et al. Farnesyltransferase inhibitor R115777 (Zarnestra, Tipifarnib) synergizes with paclitaxel to induce apoptosis and mitotic arrest and to inhibit tumor growth of multiple myeloma cells. Blood. 2005 Jun 15;105(12):4759-66.